

AD-R164 057

DEVELOPMENT OF A MODEL FOR HOT-SURFACE IGNITION OF
COMBUSTIBLE LIQUIDS(U) ADVANCED MECHANICAL TECHNOLOGY
INC NENTON MA E P DEMETRI ET AL. DEC 85

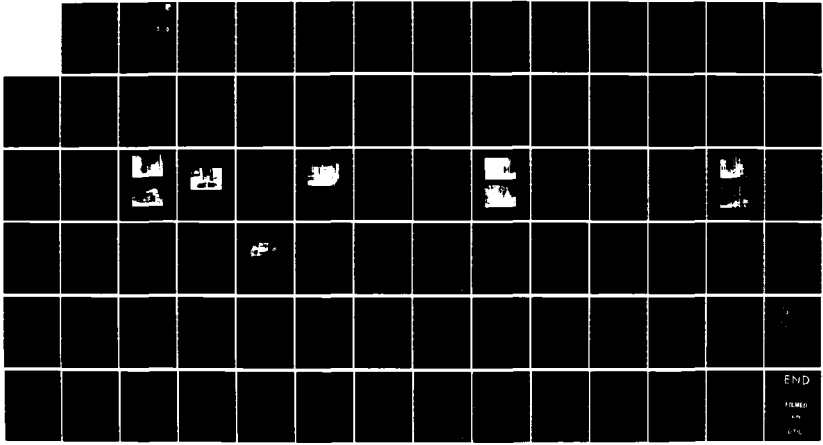
1/1

UNCLASSIFIED

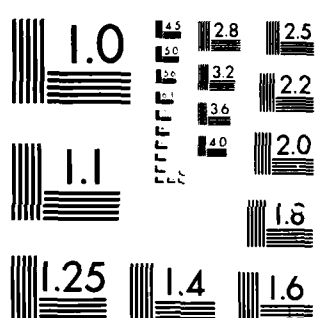
AFWAL-TR-85-2090 F33615-83-C-2380

F/G 21/2

ML



END
FILMED
BY
[illegible]



MICROCOPY RESOLUTION TEST CHART
NATIONAL BUREAU OF STANDARDS-1963-A

AD-A164 057



AFWAL-TR-85-2090

DEVELOPMENT OF A MODEL FOR HOT-SURFACE IGNITION OF COMBUSTIBLE LIQUIDS

E.P. Demetri
B.F. White

ADVANCED MECHANICAL TECHNOLOGY, INC.
141 CALIFORNIA STREET
NEWTON, MASSACHUSETTS 02158

DECEMBER 1985

DTIC
ELECTE
FEB 12 1986
S D D

FINAL REPORT FOR PERIOD OCTOBER 1983 - MAY 1984

DTIC FILE COPY

APPROVED FOR PUBLIC RELEASE; DISTRIBUTION UNLIMITED.

AERO PROPULSION LABORATORY
AIR FORCE WRIGHT AERONAUTICAL LABORATORIES
AIR FORCE SYSTEMS COMMAND
WRIGHT-PATTERSON AIR FORCE BASE, OHIO 45433

86 2 11 003

NOTICE

When Government drawings, specifications, or other data are used for any purpose other than in connection with a definitely related Government procurement operation, the United States Government thereby incurs no responsibility nor any obligation whatsoever; and the fact that the government may have formulated, furnished, or in any way supplied the said drawings, specifications, or other data, is not to be regarded by implication or otherwise as in any manner licensing the holder or any other person or corporation, or conveying any rights or permission to manufacture, use, or sell any patented invention that may in any way be related thereto.

This report has been reviewed by the Office of Public Affairs (ASD/PA) and is releasable to the National Technical Information Service (NTIS). At NTIS, it will be available to the general public, including foreign nationals.

This technical report has been reviewed and is approved for publication.



JON R. MANHEIM
Project Engineer
Fire Protection Branch
Fuels and Lubrication Division



ROBERT G. CLODFELTER, Chief
Fire Protection Branch
Fuels and Lubrication Division

FOR THE COMMANDER



ROBERT D. SHERRILL, Chief
Fuels and Lubrication Division
Aero Propulsion Laboratory

"If your address has changed, if you wish to be removed from our mailing list, or if the addressee is no longer employed by your organization please notify AFWAL/POSH, W-PAFB, OH 45433 to help us maintain a current mailing list".

Copies of this report should not be returned unless return is required by security considerations, contractual obligations, or notice on a specific document.

UNCLASSIFIED

SECURITY CLASSIFICATION OF THIS PAGE

ADA 164057

REPORT DOCUMENTATION PAGE

1a. REPORT SECURITY CLASSIFICATION UNCLASSIFIED			1b. RESTRICTIVE MARKINGS NONE			
2a. SECURITY CLASSIFICATION AUTHORITY N/A			3. DISTRIBUTION/AVAILABILITY OF REPORT APPROVED FOR PUBLIC RELEASE; DISTRIBUTION UNLIMITED			
2b. DECLASSIFICATION/DOWNGRADING SCHEDULE N/A						
4. PERFORMING ORGANIZATION REPORT NUMBER(S)			5. MONITORING ORGANIZATION REPORT NUMBER(S) AFWAL-TR-85-2090			
6a. NAME OF PERFORMING ORGANIZATION ADVANCED MECHANICAL TECHNOLOGY, INC.		6b. OFFICE SYMBOL (If applicable)	7a. NAME OF MONITORING ORGANIZATION AERO PROPULSION LABORATORY (AFWAL/POSH) AIR FORCE WRIGHT AERONAUTICAL LABORATORIES			
6c. ADDRESS (City, State and ZIP Code) NEWTON MA 02158			7b. ADDRESS (City, State and ZIP Code) WRIGHT-PATTERSON AFB OH 45433-6563			
8a. NAME OF FUNDING/SPONSORING ORGANIZATION AERO PROPULSION LABORATORY		8b. OFFICE SYMBOL (If applicable) AFWAL/POSH	9. PROCUREMENT INSTRUMENT IDENTIFICATION NUMBER F33615-83-C-2380			
8c. ADDRESS (City, State and ZIP Code) WRIGHT-PATTERSON AFB OH 45433-6563			10. SOURCE OF FUNDING NOS.			
			PROGRAM ELEMENT NO. 65502F	PROJECT NO. 3005	TASK NO. 20	WORK UNIT NO. 09
11. TITLE (Include Security Classification) DEVELOPMENT OF A MODEL FOR HOT-SURFACE IGNITION OF COMBUSTIBLE LIQUIDS						
12. PERSONAL AUTHOR(S) E.P. DEMETRI AND B.F. WHITE						
13a. TYPE OF REPORT FINAL		13b. TIME COVERED FROM OCT 83 TO MAY 84		14. DATE OF REPORT (Yr., Mo., Day) December 1985		15. PAGE COUNT 78
16. SUPPLEMENTARY NOTATION						
17. COSATI CODES			18. SUBJECT TERMS (Continue on reverse if necessary and identify by block number)			
FIELD	GROUP	SUB. GR.	HOT-SURFACE IGNITION, COMBUSTION, FUEL			
21	02					
21	04					
19. ABSTRACT (Continue on reverse if necessary and identify by block number) There are many military systems requiring the storage and use of combustible liquids which can accidentally contact a hot surface resulting in a potential fire or explosion hazard. The optimum design of appropriate safety measures is severely hampered by the fact that the thermal ignition of liquids is not well understood. A research study has been conducted to develop and experimentally verify a model of the hot-surface ignition phenomenon for combustible liquids. A large number of parametric tests have been performed to measure surface ignition temperature and delay time for a wide variety of conditions. A simple analytical model has been derived and successfully applied in correlating the experimental data. The results obtained in the study demonstrate the utility of the analytical and experimental techniques which have been developed.						
20. DISTRIBUTION/AVAILABILITY OF ABSTRACT UNCLASSIFIED/UNLIMITED <input checked="" type="checkbox"/> SAME AS RPT. <input type="checkbox"/> DTIC USERS <input type="checkbox"/>			21. ABSTRACT SECURITY CLASSIFICATION UNCLASSIFIED			
22a. NAME OF RESPONSIBLE INDIVIDUAL JON R. MANHEIM			22b. TELEPHONE NUMBER (Include Area Code) (513) 255-6980		22c. OFFICE SYMBOL AFWAL/POSH	

U.S. DEPARTMENT OF ENERGY
SMALL BUSINESS INNOVATION RESEARCH PROGRAM
PHASE I—FY 1983
PROJECT SUMMARY

FOR DOE USE ONLY

Program Office	TTM	Proposal No.	Topic No.
----------------	-----	--------------	-----------

TO BE COMPLETED BY PROPOSER

Name and Address of Proposer

Advanced Mechanical Technology, Inc.
141 California Street
Newton, Massachusetts 02158

Name and Title of Principal Investigator

Elia P. Demetri, Manager Thermal Systems

Title of Project

Development of a Model for Hot-Surface Ignition of Combustible Liquids

Technical Abstract (Limit to two hundred words)

There are many military systems requiring the storage and use of combustible liquids which can accidentally contact a hot surface resulting in a potential fire or explosion hazard. The optimum design of appropriate safety measures is severely hampered by the fact that the thermal ignition of liquids is not well understood. A research study has been conducted to develop and experimentally verify a model of the hot-surface ignition phenomenon for combustible liquids. A large number of parametric tests have been performed to measure surface ignition temperature and delay time for a wide variety of conditions. A simple analytical model has been derived and successfully applied in correlating the experimental data. The results obtained in the study demonstrate the utility of the analytical and experimental techniques which have been developed.

Anticipated Results/Potential Commercial Applications of the Research

The research has resulted in a general ignition model which offers significant promise as a practical safety design and analysis tool for dealing with the potential hazards associated with combustible liquids. Eventual application of the model to Air Force systems will greatly increase the confidence level in selecting optimum safety measures and will reduce the development effort, cost, and complexity of the required design. It is anticipated that safety testing and analysis based on the developed procedures and experimental facility can ultimately be offered as a commercial service to interested users and suppliers of combustible liquids.

ACKNOWLEDGMENTS

The authors wish to express their gratitude to Dr. Jon R. Manheim of Wright Patterson for his valuable guidance in maintaining the proper focus for the study. A special note of thanks is also due to Professor Normand M. Laurendeau of Purdue University for his very helpful comments and suggestions as a consultant throughout the course of the program.

Accession For	
NTIS CRA&I	<input checked="" type="checkbox"/>
DTIC TAB	<input type="checkbox"/>
Unannounced	<input type="checkbox"/>
Justification	
By	
Distribution /	
Availability Codes	
Dist	Avail and/or Special
A-1	

TABLE OF CONTENTS

		<u>PAGE</u>
1.	INTRODUCTION	1
	1.1 Background	1
	1.2 Program Objectives	2
	1.3 Technical Approach	2
2.	DEVELOPMENT OF PRELIMINARY IGNITION MODEL	4
	2.1 Basis of Model	4
	2.2 Fuel Vaporization	6
	2.3 Fuel/Air Mixing	10
	2.4 Fuel Oxidation	12
	2.4.1 Steady-State Model	14
	2.4.2 Transient Model	17
3.	IGNITION TEST FACILITY AND PROCEDURES	19
	3.1 Overview of Test Apparatus	19
	3.2 Reactor Design	19
	3.3 Control of Mixture Composition	24
	3.3.1 Vaporized Fuel and Air	24
	3.3.2 Liquid Fuel and Air	28
	3.4 Heating Circuit	31
	3.5 Foil Temperature Measurement	35
	3.6 Test Procedures	38
	3.6.1 Vaporized Fuel Ignition Tests	38
	3.6.2 Liquid Fuel Ignition Tests	39
4.	ANALYSIS AND CORRELATION OF TEST RESULTS	43
	4.1 Parametric Experimental Investigation	43
	4.2 Correlating Equations	45
	4.2.1 Correlating Equation for Ignition Temperature	46
	4.2.2 Correlating Equations for Ignition Delay Time	47
	4.3 Ignition of Vaporized Fuel/Air Mixtures	48
	4.3.1 General Observations	48
	4.3.2 Ignition Temperature	51
	4.3.3 Vapor Phase Ignition Delay Time	56
	4.4 Ignition of Liquid Fuel/Air Mixtures	58
	4.4.1 Spray Characteristics	58
	4.4.2 Details of Ignition Process	60
	4.4.3 Correlation of Spray Ignition Delay Time ..	63
	4.5 Model Assessment	66
5.	CONCLUSIONS	69
6.	RECOMMENDATIONS	71
7.	REFERENCES	72

LIST OF FIGURES

<u>FIGURE</u>		<u>PAGE</u>
1	Qualitative Illustration of Effect of Liquid Phase on Ignition Delay	5
2	Schematic of Fuel Droplet Evaporation Model	7
3	Temperature Profiles Near Heated Surface Surrounded by Flammable Mixture	13
4	Overall Schematic of Hot-Surface Ignition Test Loop ..	20
5	Components of test Facility	21
6	Reactor Configuration for Vaporized Fuel Tests	22
7	Closeup View of Test Reactor	23
8	Schematic of Saturating Chamber	25
9	Saturating Chamber Used in Preparing Vaporized Fuel/Air Mixtures	26
10	Schematic of Liquid Fuel Injection Tube	29
11	Liquid Fuel Injection Assembly	30
12	Schematic of Foil Heating Circuit	32
13	Foil Mounting Arrangement in Reactor	33
14	Typical Time-Temperature History for 4.76 mm Foil in Air	34
15	Typical Foil/Thermocouple Assembly for Calibration of Optical Temperature Measurement Technique	36
16	Calibration of Photo-Optical Temperature Measurement Technique	37
17	Typical Test Results for Vaporized Hexane/Air Mixture .	40
18	Typical Test Results for Octane Liquid Spray Ignition .	42
19	Typical Effect of Hot-Surface Temperature on Ignition Condition	49
20	Apparent Effect of Surface Reaction on Preignition Temperature Profile	50
21	Correlation of Ignition Temperature Data for Hexane Vapor	53
22	Variation of Ignition Temperature with Equivalence Ratio and Foil Size for Hexane Vapor	54
23	Comparison of Ignition Temperature for Hexane and Octane with 4.76 mm Foil	55
24	Correlation of Vapor Phase Ignition Delay Time for Hexane with 9.52 mm Foil	57
25	Effect of Surface Size on Ignition Delay Time for Hexane	59
26	Typical Effect of Hot-Surface Temperature on Spray Ignition Delay Time for Octane	61
27	Typical Effect of Drop Size on Spray Ignition Delay Time for Octane	62
28	Correlation of Octane Spray Ignition Test Results for 0.6 GPH Atomizer	64
29	Correlation of Octane Spray Ignition Test Results for 2.75 GPH Atomizer	65
30	Variation of Octane Spray Ignition Delay Time with Surface Temperature and Drop Size	68

LIST OF TABLES

<u>TABLE</u>		<u>PAGE</u>
1	Summary of Experimental Ignition Results for Mixtures of Vaporized Fuel and Air	44
2	Summary of Experimental Ignition Results for Sprays of Liquid Octane in Air	67

1. INTRODUCTION

1.1 Background

There are a large number of military applications requiring the storage and use of combustible liquids such as fuels, lubricants, and hydraulic fluids. These applications include both stationary and mobile operations. Military aircraft represent a prime example which is particularly relevant to Air Force applications. Other examples include ground-based service vehicles, fuel storage facilities, and power generating equipment. In any of these systems, a variety of combat and non-combat scenarios are possible which could result in contact of the combustible liquid with a hot surface. The hot surface can either be due to friction generated during an accident or can exist as a result of normal system operation (an engine tailpipe, for example). In any event, the accidental release of combustible liquid can result in a fire and/or explosion, if the proper conditions exist.

Because of the potential hazard to personnel and equipment, it is necessary to incorporate appropriate safety measures in the design of the systems to minimize the probability of accidental ignition of any combustible fluids. Unfortunately, the process of ignition by a hot surface is not very well understood and relatively little information is available, particularly for the case of liquids. The required safety precautions for any given system are then typically developed on a purely empirical basis or by applying general rules of thumb. This is often a time-consuming, expensive and inaccurate approach. Consequently, the resulting safeguards are either inadequate leading to undue risk or are overdesigned leading to systems which are larger, more complicated and costlier than necessary.

The research program described in this report was conducted to address the specific problem of the current lack of understanding of the hot-surface ignition phenomenon as related to combustible liquids. The study was aimed at expanding the relevant technology base in the subject area so as to span the existing gap in the state-of-the-art. The effort conducted was sponsored by the Department of the Air Force under Contract

No. F33615-83-C-2380 as a Phase I study in the overall Defense Small Business Innovation Research (SBIR) Program.

1.2 Program Objectives

The principal goal of the Phase I investigation was to develop and experimentally verify the feasibility of an ignition model which adequately represents the important mechanisms involved in the hot-surface ignition of combustible liquids. The specific objectives of the research effort required to attain this goal were as follows:

- To formulate an initial ignition model which accounts for the anticipated major effects.
- To conduct a series of controlled ignition experiments with liquid fuels for the purpose of obtaining the test data necessary to demonstrate the feasibility of the analytical approach.
- To refine the model as necessary to correlate the test results and obtain satisfactory agreement between theory and experiment.

It was intended that the results obtained in the initial investigation would provide a firm basis for extending the capabilities of the model and adding to the body of useful test data in subsequent efforts. The ultimate aim of these efforts would be to develop a detailed practical tool which could be applied with confidence in the design and analysis of optimum safety measures for systems involving combustible liquids.

1.3 Technical Approach

The overall research effort conducted consisted of a combined analytical and laboratory-scale experimental investigation of the ignition of combustible liquids by contact with hot surfaces. The general approach selected was based on modifying and extending procedures developed by Laurendeau and Caron (Refs. 1, 2, and 3) in a previous study which focused on methane/air mixtures and included a critical review of available literature on the general process of thermal ignition. In this original study a simple analytical model was derived for predicting the ignition surface temperature and delay time for the case of vaporized

fuel/air mixtures. As part of the study, a laboratory apparatus was designed and constructed for the purpose of conducting controlled tests of the thermal ignition phenomenon. The test results obtained with this apparatus provided experimental confirmation of the basic utility of the vapor model in correlating ignition surface temperature data.

In the current program, a corresponding model was developed for the case of liquid fuel ignition. The derivation of the model was based on assuming that the three major rate processes involved in ignition (fuel vaporization, mixing, and chemical reaction) occur sequentially rather than simultaneously. Appropriate equations were developed for the characteristic times associated with vaporization and mixing. Combining these with a modified version of the transient vapor ignition model (Ref. 1) resulted in a comparatively simple relationship which expresses the total ignition delay time as a function of ambient conditions, fuel properties, composition of the fuel/air mixture, and the temperature and geometry of the heated surface.

The basic approach used in conducting the experimental investigation consisted of exposing a combustible fuel/air mixture to an electrically heated metal foil contained within a transparent cylindrical reactor. For a given mixture composition, a number of different foil temperatures were investigated bracketing the specific value required to achieve ignition under each set of test conditions. The relevant features of the ignition process were determined by optically monitoring the time-temperature history of the foil using a phototransistor sensitive to infrared radiation connected to a storage oscilloscope.

A comprehensive set of parametric tests including both vaporized and liquid fuels was performed. The preliminary ignition model was applied in obtaining correlations of the experimental data. Appropriate empirical constants were evaluated and the model was modified as necessary to achieve satisfactory agreement between theoretically predicted and experimentally observed variations in the major ignition criteria. The analytical and experimental results obtained in the program are presented and discussed in detail in the remainder of this report.

2. DEVELOPMENT OF PRELIMINARY IGNITION MODEL

2.1 Basis of Model

The ignition of a combustible mixture of liquid fuel and air is a transient phenomenon which involves three major rate processes:

1. Vaporization of the liquid fuel
2. Mixing of the fuel vapor with air
3. Reaction of the vaporized fuel and air

In the case of hot-surface ignition, all of these processes are initiated and driven by heat transfer from the surface to the surrounding combustible mixture. The time required to achieve ignition is then dependent on the interrelationships among the rates of the simultaneously occurring processes of heat transfer, vaporization, mixing, and reaction.

The primary objective in developing the initial model was to provide a simple analytical framework for the purposes of interpreting the test data and gaining insights into the relative importance of different effects. In order to obtain a useful model, it was necessary to make a number of simplifying assumptions, the principal one being that the three major rate processes occur sequentially rather than simultaneously. With this assumption the overall ignition delay time (τ_I) can be expressed as:

$$\tau_I = \tau_V + \tau_M + \tau_R \quad (1)$$

where τ_V , τ_M , and τ_R are the characteristic times for vaporization, mixing, and reaction. By decoupling these processes, an appropriate expression can be derived for each characteristic time. The hypothetical variation of ignition delay time with temperature would then be expected to be as illustrated in Figure 1.

The preliminary model described below was developed for the specific case where the fuel is in the form of liquid droplets. This case is not only of practical interest in potential accident scenarios, but also provides a reasonably simple basis for experimentally investigating the

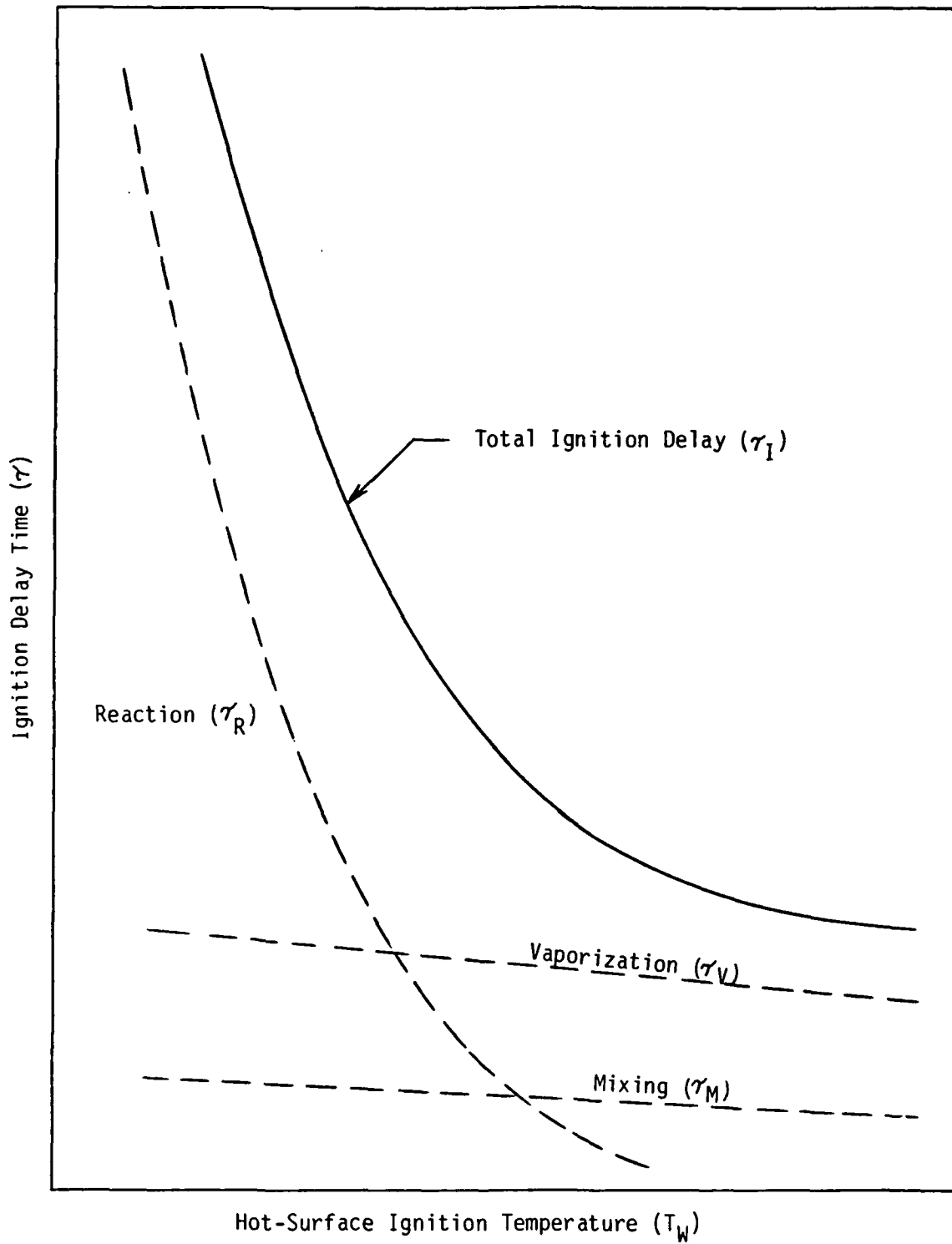


Figure 1. QUALITATIVE ILLUSTRATION OF EFFECT OF LIQUID PHASE ON IGNITION DELAY

importance of various parameters. The basic model can be extended to more complex situations, such as fuel jet impingement on a heated surface, in a fairly straightforward manner in subsequent more comprehensive investigations of the phenomenon.

2.2 Fuel Vaporization

The liquid fuel is assumed to exist as a monodisperse spray distributed uniformly throughout the volume of air. Each drop is considered as centered in a cubical "cell" of air whose sides are of length δ :

$$\delta = \left(\frac{\rho_L}{6\rho X_F} \right)^{1/3} a_0 \quad (2)$$

where

ρ_L = liquid fuel molar density

X_F = mole fraction of fuel

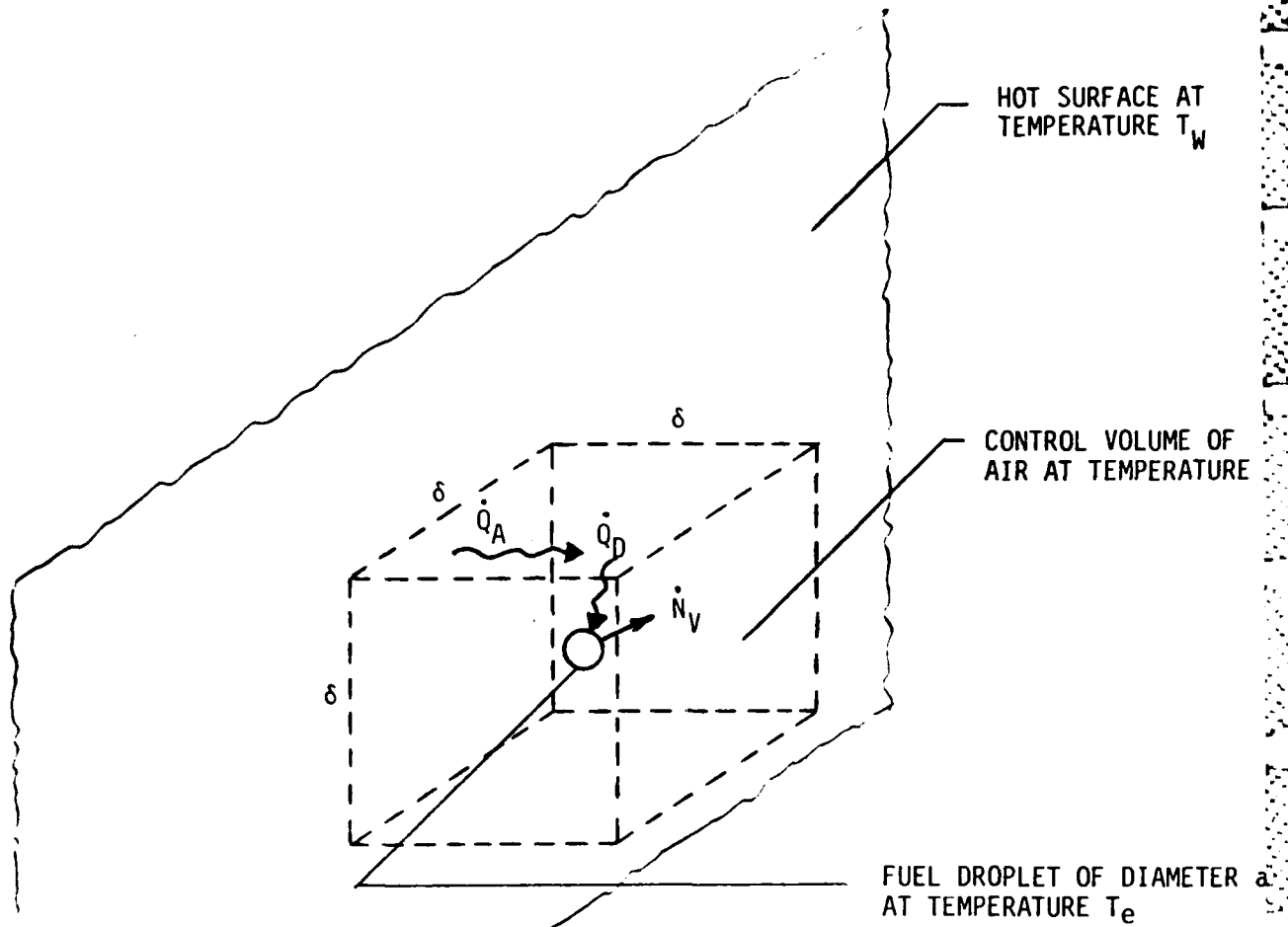
a_0 = initial drop diameter

and ρ is the air molar density evaluated at the geometric mean temperature ($\bar{T} = \sqrt{T_e T_w}$):

$$\rho = \frac{\rho_e}{(T_w/T_e)^{1/2}} \quad (3)$$

$$\rho_e = \frac{P}{RT_e} \quad (4)$$

with P = ambient pressure and R = universal gas constant. The vaporization of fuel due to heat transfer from a hot surface immersed in the combustible mixture can then be approximately modeled by considering a portion of the surface with a single cell adjacent to it as shown in Figure 2.



NOTES:

\dot{Q}_A = Heat Transfer Rate from Surface to Air

\dot{Q}_D = Heat Transfer Rate from Air to Droplet

\dot{N}_V = Vapor Generation Rate

Figure 2. SCHEMATIC OF FUEL DROPLET EVAPORATION MODEL

During the evaporation period it is assumed that direct radiation heat transfer from the wall to the drop is negligible and a state of equilibrium exists such that:

$$\dot{Q}_D = \dot{Q}_A \quad (5)$$

where:

$$\dot{Q}_D = h_D(\pi a^2)(T_A - T_e) \quad (6)$$

$$\dot{Q}_A = h_W \delta^2 (T_W - T_A) \quad (7)$$

The heat-transfer coefficients, h_D and h_W , can be expressed in terms of the corresponding Nusselt numbers as follows:

$$h_D = \frac{k \text{Nu}_D}{a} \quad (8)$$

$$h_W = \frac{k \text{Nu}_W}{L} \quad (9)$$

where

k = thermal conductivity of air

L = characteristic dimension of hot surface

The vaporization rate (\dot{N}_V) is related to the rate of change of drop diameter and \dot{Q}_D as follows:

$$\dot{N}_V = \frac{d}{dt} \left(\frac{\pi}{6} \rho_L a^3 \right) \approx \frac{\dot{Q}_D}{\lambda} \quad (10)$$

where λ = latent heat. By combining Equations 3 through 8 and eliminating T_A , the following differential equation is obtained:

$$- \left[a + \pi \left(\frac{\text{Nu}_D}{\text{Nu}_W} \right) \left(\frac{L}{\delta^2} \right) a^2 \right] \frac{da}{dt} = \frac{2k \text{Nu}_D (T_W - T_e)}{\lambda \rho_L} \quad (11)$$

Integrating from the initial drop diameter $a = a_0$ to $a = 0$ gives the following final expression for evaporation time:

$$\tau_V = \tau_{V,REF} \left(1 + \beta \frac{L}{a_0 \theta_W^{1/3}} \right) \quad (12)$$

where:

$$\tau_{V,REF} = \left(\frac{\lambda \rho_L}{4kT_e \text{Nu}_D} \right) \frac{a_0^2}{(\theta_W - 1)} \quad (13)$$

$$\beta = \left(\frac{2\pi}{3} \right) \left(\frac{6\rho_e \chi_F}{\pi \rho_L} \right)^{2/3} \frac{\text{Nu}_D}{\text{Nu}_W} \quad (14)$$

and θ_W is the surface temperature nondimensionalized with respect to the ambient temperature:

$$\theta_W = \frac{T_W}{T_e} \quad (15)$$

It is of interest to note that $\tau_{V,REF}$ corresponds to the value given by the classic " D^2 law" for evaporation of droplets in a free stream at temperature T_W . Equation 12 predicts that the actual vaporization time will be greater than this value by an amount which, as one would intuitively expect, depends on the relative characteristics of the heat transfer at the hot surface in comparison to the droplets in the free stream. A reasonable approximation is that the droplets are stagnant with respect to the surrounding air in which case $\text{Nu}_D \approx 2$ (Ref. 4). The corresponding value of Nu_W can be determined from conventional empirical expressions for different heat-transfer situations. The appropriate relationships for three cases of practical interest are as follows:

1. For stagnant conditions,

$$\text{Nu}_W = \text{constant} \quad (16)$$

2. For laminar natural convection from a vertical surface in air (Ref. 5),

$$Nu_W \approx \frac{C_{NC} T_e^{1/4}}{k} (\theta_W - 1)^{1/4} L^{3/4} \quad (17)$$

where C_{NC} is an empirical constant.

3. For laminar flow forced convection past a flat plate (Ref. 6),

$$Nu_W = C_{FC} Pr^{1/3} \left(\frac{\rho_e}{\mu} \right)^{1/2} \frac{(LU)^{1/2}}{\theta_W^{1/4}} \quad (18)$$

where

C_{FC} = empirical constant

Pr = Prandtl number

U = free-stream velocity

μ = air viscosity

Combination of Equations 12-18 results in three different expressions for the vaporization time depending on the prevailing mode of heat transfer at the hot surface. Obviously, a similar procedure could be followed in extending the basic model to other heat-transfer or geometric conditions.

2.3 Fuel/Air Mixing

In keeping with the original assumption regarding the decoupling of the rate processes, the mixing is considered to begin after all of the fuel has evaporated. At this point in time, it is assumed that the fuel contained in each droplet is in the form of a sphere of vapor of diameter $a_{v,0}$:

$$a_{v,0} = \left(\frac{\rho_L}{\rho} \right)^{1/3} a_0 \quad (19)$$

Although this assumption is somewhat artificial, it is a useful fiction which results in a reasonable expression for the characteristic mixing time.

The rate at which the vapor mixes into the free stream (\dot{N}_M) is given by the expression for turbulent diffusion from the surface of the sphere:

$$\dot{N}_M = (\pi a_V^2) \rho k_C (1-X) \quad (20)$$

where

k_C = mass-transfer coefficient

X = mole fraction of vapor in the free stream

From the analogy between heat transfer and mass transfer:

$$k_C = \frac{D_V}{a_V} Nu_D \quad (21)$$

where D_V = diffusion coefficient for fuel vapor in air. Recognizing that:

$$\dot{N}_M = -\rho \frac{\pi}{2} a_V^2 \frac{dX}{dt} \quad (22)$$

the above set of equations can be solved to give:

$$-\left(\frac{a_V}{(X_0/X_F) + (a_V/a_{V,0})^3} \right) \frac{dX}{dt} = \frac{2D_V Nu_D X_F}{a_{V,0}^2} \quad (23)$$

where

X_F = overall mole fraction of fuel

X_0 = overall mole fraction of air

Integrating from $a_V = a_{V,0}$ to $a_V = 0$ gives the following final expression for the characteristic mixing time:

$$\tau_M = \frac{(\rho_L/\rho_e)^{2/3}}{6D_V Nu_D} \frac{F(C_X)}{X_F C_X} \frac{a_0^2}{\theta_W^{1/3}} \quad (24)$$

where C_X and $F(C_X)$ are functions of the overall mixture composition defined as:

$$C_X = (X_O/X_F)^{1/3}$$
$$F(C_X) = \frac{1}{2} \ln \left(\frac{C_X^2 - C_X + 1}{(C_X + 1)^2} \right) + \sqrt{3} \left[\tan^{-1} \left(\frac{2 - C_X}{C_X \sqrt{3}} \right) + \frac{\pi}{6} \right] \quad (25)$$

2.4 Fuel Oxidation

The selected analytical methods for representing the chemical reaction of vaporized fuel and air are based on the theoretical procedures developed by Laurendeau (Ref. 1). This results in two separate but related models of the vapor ignition process. One is a steady-state version which predicts the surface temperature required for ignition. The steady-state model should be useful for correlating ignition temperature data not only for vaporized fuel but also, with some modification, for cases where the fuel is initially in a liquid state. The second form of the model is a transient version which predicts the delay time associated with the vapor phase ignition process.

The theoretical development is based on the principal assumption that the so-called Van't Hoff criterion defines the conditions corresponding to the initiation of ignition. This is illustrated by the hypothetical temperature profiles shown in Figure 3. Curve 1 represents conductive heat transfer from the surface into the surrounding boundary layer prior to ignition, while Curve 3 represents heat transfer to the surface from the hot combustion products after ignition. Curve 2 defines the Van't Hoff criterion which simply states that at the point of ignition the rate of heat loss to the surroundings is equal to the rate of heat gain due to chemical reaction.

The other major assumptions are as follows:

- No reactant depletion occurs until ignition.
- Chemical reaction occurs in a stagnant film in the immediate vicinity of the hot surface.

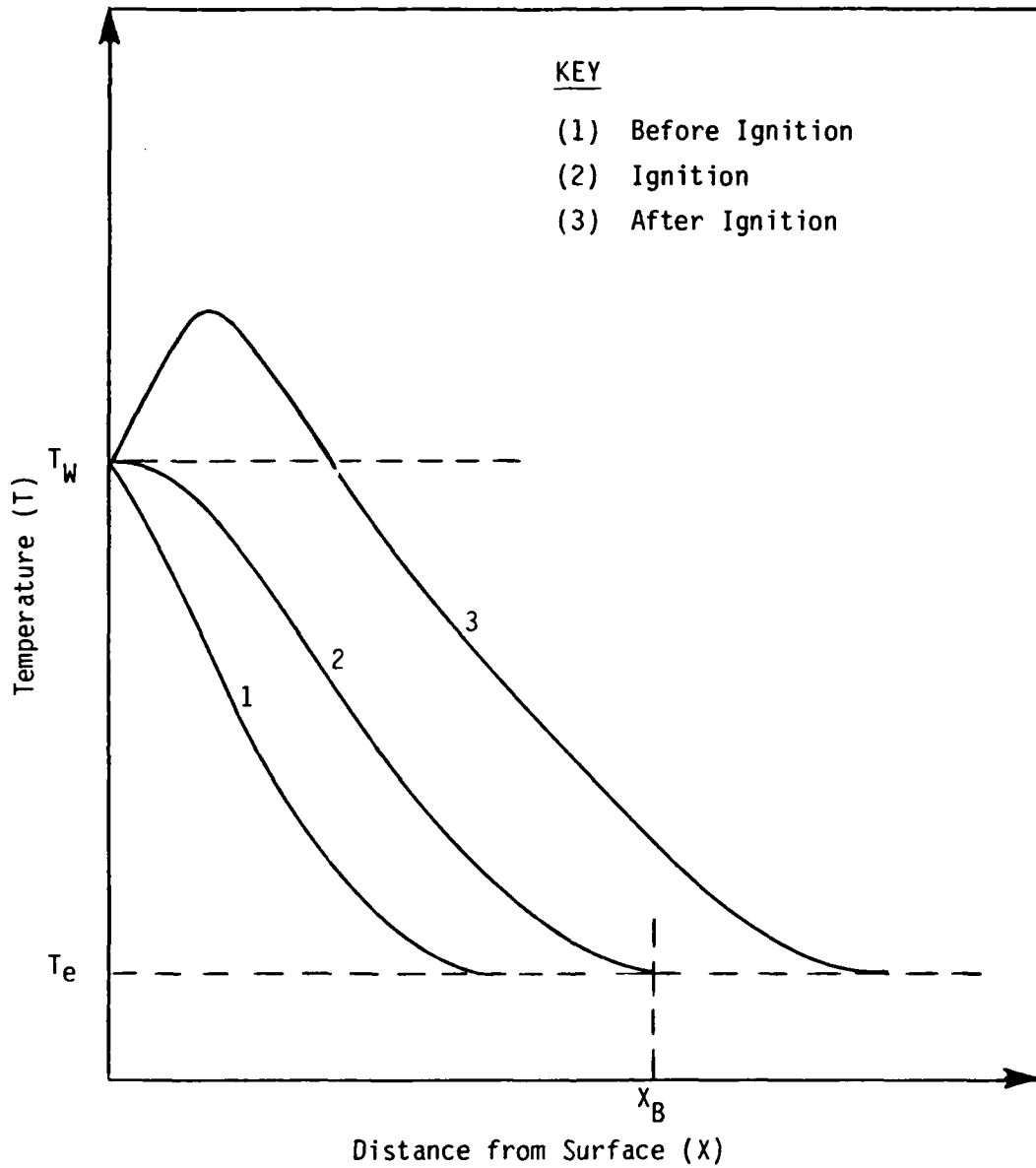


Figure 3. TEMPERATURE PROFILES NEAR HEATED SURFACE SURROUNDED BY FLAMMABLE MIXTURE

- Heat transfer is independent of chemical reaction.
- Chemical kinetics can be represented by an Arrhenius expression for a one-step global reaction; that is:

$$r_F = X_F^{m_F} X_O^{m_O} \rho_e^n A \exp\left(-\frac{E}{RT}\right) \quad (26)$$

where r_F is molar reaction rate, A is the frequency factor, E is the activation energy, m_F and m_O are the partial orders with respect to fuel and oxidizer, and $n = m_F + m_O$ is the overall reaction order.

- Physical properties are constant.

The theoretical development of the ignition models based on these assumptions is described in detail in References 1 and 3. The relevant features of the derivations, including in particular the modifications which have been made in the current modeling effort, are presented below along with the resulting analytical expressions.

2.4.1 Steady-State Model

The heat transfer rate at the surface due to chemical reaction alone can be determined by integrating the energy conservation equation for a reacting medium with the following boundary conditions:

$$\frac{dT}{dX} = \left(\frac{dT}{dX}\right)_W \text{ @ } T = T_W$$

$$\frac{dT}{dX} = \left(\frac{dT}{dX}\right)_e \text{ @ } T = T_e$$

This results in a temperature profile similar to Curve 3 of Figure 3 and a differential equation of the following form:

$$\left(\frac{dT}{dX}\right)_W^2 - \left(\frac{dT}{dX}\right)_e^2 = f(T_e, T_W) \quad (27)$$

In order to obtain a solution it is necessary to assume some relationship between the two slopes. The simplest approximation is to assume that

$(dT/dX)_e^2 \approx 2(dT/dX)_W^2$. Although this is somewhat arbitrary it has relatively little impact from a practical standpoint since it affects only the value of any empirical constant necessary to apply the model in correlating test data. With this simplifying assumption, the heat-transfer rate due to chemical reaction is given by:

$$\dot{q}_{\text{CHEM}} = \left[2kAX_F^{m_F} X_O^{m_O} Q_e^n \left(\frac{T_e}{T_W}\right)^{n/2} \left(\frac{RT_W^2}{E}\right) \exp(-E/RT_W) \right]^{1/2} \quad (28)$$

where Q is the heat of combustion.

To complete the analysis an expression is needed for the rate of heat loss from the surface in the absence of reaction. This is simply,

$$\dot{q}_{\text{LOSS}} = \frac{k \text{Nu}_W}{L} (T_W - T_e) \quad (29)$$

Applying the Van't Hoff criterion,

$$\dot{q}_{\text{LOSS}} = \dot{q}_{\text{CHEM}} \quad (30)$$

results in the following expression of the ignition criterion:

$$F_\theta \exp(E^*/\theta_W) = \frac{2D_1 D_2}{E^*} \quad (31)$$

In this equation, θ_W is the nondimensional surface temperature given by Equation 15, F_θ is defined as,

$$F_\theta = \left(\frac{\theta_W - 1}{\theta_W}\right)^2 \theta_W^{n/2} \quad (32)$$

E^* is the nondimensional activation energy,

$$E^* = \frac{E/R}{T_e} \quad (33)$$

and D_1 , D_2 are Damkohler numbers of the first and second kind,

$$D_1 = A \frac{n-1}{\rho_e} X_o^{m_0} \left(\frac{L^2}{\alpha \text{Nu}_W} \right) \quad (34)$$

$$D_2 = \frac{X_F^{m_F} Q}{C_p T_e} \quad (35)$$

where α is the thermal diffusivity,

$$\alpha = \frac{k}{\rho_e C_p} \quad (36)$$

and C_p is the specific heat at constant pressure.

A more convenient expression for the ignition criterion can be obtained by reformulating Equation 31 to give:

$$\frac{L}{\text{Nu}_W} = (\alpha \tau_{SS})^{1/2} \quad (37)$$

where τ_{SS} is a characteristic time given by the following equation:

$$\tau_{SS} = \left(\frac{E^* F \theta}{2 A D_2 \frac{n-1}{\rho_e} X_o^{m_0}} \right) \exp (E^* / \theta_W) \quad (38)$$

As discussed previously in the derivation of the vaporization time constant, appropriate empirical expressions for Nu_W are available for different modes of heat transfer. These can be substituted in Equation 37 and solved to obtain explicit relationships between the characteristic surface dimension L and ignition temperature. For purposes of illustration it is of interest to examine the relationships for a given fuel, composition, and ambient temperature. Recognizing that the exponential term dominates the temperature effect it is found that for stagnant conditions:

$$L \propto \tau_{SS}^{1/2} \alpha \exp (E^* / 2 \theta_W) \quad (39)$$

for natural convection:

$$L \alpha \tau_{SS}^2 \propto \exp(2E^*/\theta_W) \quad (40)$$

and for forced convection:

$$L \alpha \tau_{SS} \propto \exp(E^*/\theta_W) \quad (41)$$

These forms are useful in suggesting methods of presenting and correlating ignition temperature test data as will be subsequently demonstrated.

2.4.2 Transient Model

In the original development described in Reference 1, a transient analysis was performed to derive an expression for the vapor-phase ignition delay time, τ_R . The analysis was based on representing the transient temperature profile prior to ignition by the expression for a semi-infinite slab suddenly exposed to a high temperature on one side. Implicit in this approach is the assumption that the heat-transfer coefficient is infinite. Consequently, the resulting model is strictly valid only for the case of stagnant conditions where thermal diffusion controls. In order to account approximately for the more practical situation where convective heat transfer dominates, the original approach has been modified. The modification consists of assuming that the thermal conductivity appearing in the expression for the transient temperature profile can be replaced by an "effective conductivity" defined as:

$$k_{EFF} = Nu_W k \quad (42)$$

With this approximation, the transient heat loss rate is given by:

$$q_{LOSS} = -Nu_W k \left(\frac{dT}{dX} \right)_W = \left(\frac{Nu_W}{\pi \alpha t} \right)^{1/2} k (T_W - T_e) \quad (43)$$

Applying the Van't Hoff criterion at $t = \tau_R$ by combining Equations 28, 30, 38, and 43, the following expression is obtained:

$$\tau_R = \frac{Nu_W}{\pi} \tau_{SS} \quad (44)$$

As discussed previously, empirical expressions for Nu_W can be used in conjunction with Equations 37 and 44 to eliminate L and arrive at relationships for τ_R as functions of surface temperature. Analogous to the results obtained with the steady-state model for the case of a given fuel, composition, and ambient temperature it can be shown that for stagnant conditions,

$$\tau_R \propto \tau_{SS} \propto \exp(E^*/\theta_W) \quad (45)$$

for natural convection,

$$\tau_R \propto \tau_{SS}^{5/2} \propto \exp(2.5 E^*/\theta_W) \quad (46)$$

and for forced convection,

$$\tau_R \propto U \tau_{SS}^{3/2} \propto U \exp(1.5 E^*/\theta_W) \quad (47)$$

Again as in the case of the steady-state model these expressions are useful in suggesting approaches for correlating test data.

3. IGNITION TEST FACILITY AND PROCEDURES

3.1 Overview of Test Apparatus

The selected experimental approach is an extension of the method used successfully by Laurendeau and Caron (Ref. 2) for thermal ignition testing of methane. The basic approach consists of exposing a combustible mixture to an electrically-heated foil contained within a transparent cylindrical reactor. The foil is heated to different temperature levels in successive tests to determine the conditions required to achieve ignition. The relevant features of the ignition process are observed and measured by monitoring the time-temperature history of the foil using a fast-response optical technique.

The overall test apparatus which was constructed and used in conducting the parametric experimental investigation is shown schematically in Figure 4. Photographs of the major components are given in Figure 5. As indicated, the apparatus provided the capability of testing mixtures of vaporized or liquid fuel and air. A fast-acting nitrogen purge system allowed rapid quenching of any flame if necessary following ignition.

3.2 Reactor Design

One of the principal components of the system is the reactor which is installed in a ventilated hood for safety during testing. The major design features of the reactor are shown in the sketch given in Figure 6 and the photograph given in Figure 7. The particular configuration shown is the one used in conducting tests with vaporized fuel. In this case, the fuel/air mixture flows into the base of the reactor and passes through a shallow bed of glass beads and a sintered metal plate. This assembly acts both as a flow straightener and a flame arrestor. The top cover of the reactor is a loosely-fitting beveled disk which prevents confinement of the hot combustion gases when ignition is achieved.

For tests involving liquid fuel, the sintered plate and layer of glass beads were removed. In addition, the fitting in the top cover was

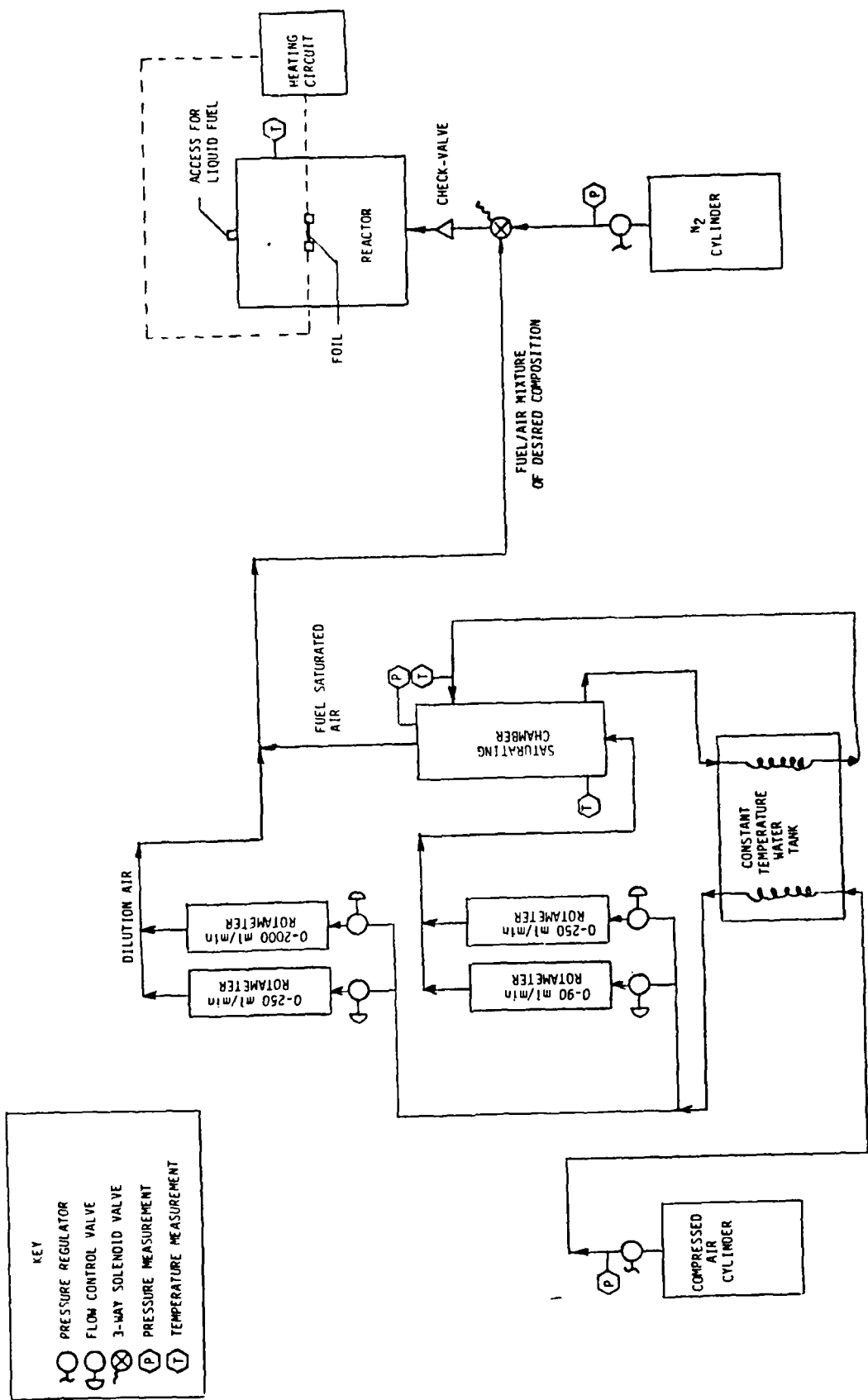


Figure 4. OVERALL SCHEMATIC OF HOT-SURFACE IGNITION TEST LOOP

- KEY
- PRESSURE REGULATOR
 - FLOW CONTROL VALVE
 - 3-WAY SOLENOID VALVE
 - PRESSURE MEASUREMENT
 - TEMPERATURE MEASUREMENT

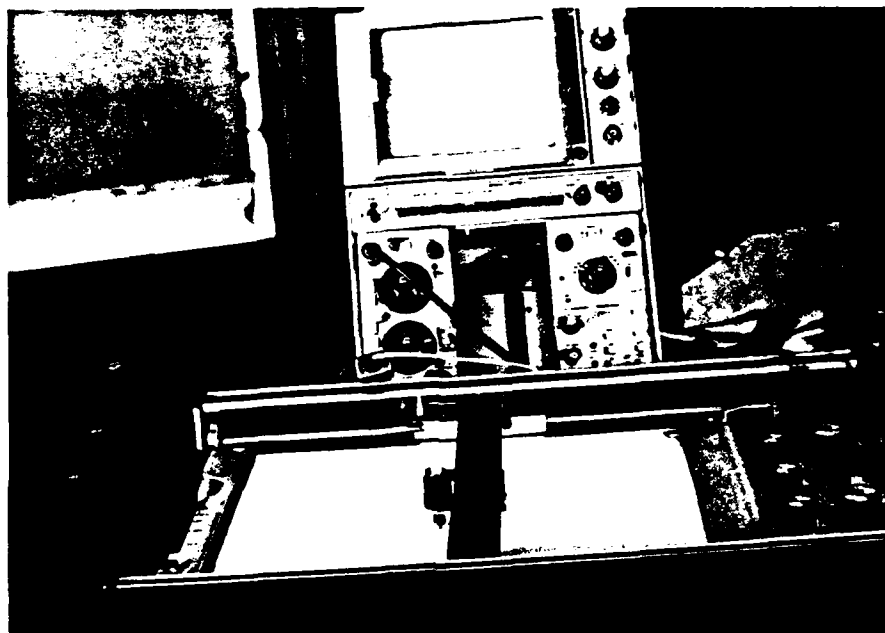


(a) From Left to Right: Saturating Chamber,
Flow Control Solenoid Valve, Reactor



(b) From Left to Right: Heating Circuit Power Supply,
Control Panel and Instrument Displays, Bank of
Rotameters

Figure 5. COMPONENTS OF TEST FACILITY



(c) Storage Oscilloscope and X-Y Plotter

Figure 5 (continued) COMPONENTS OF TEST FACILITY

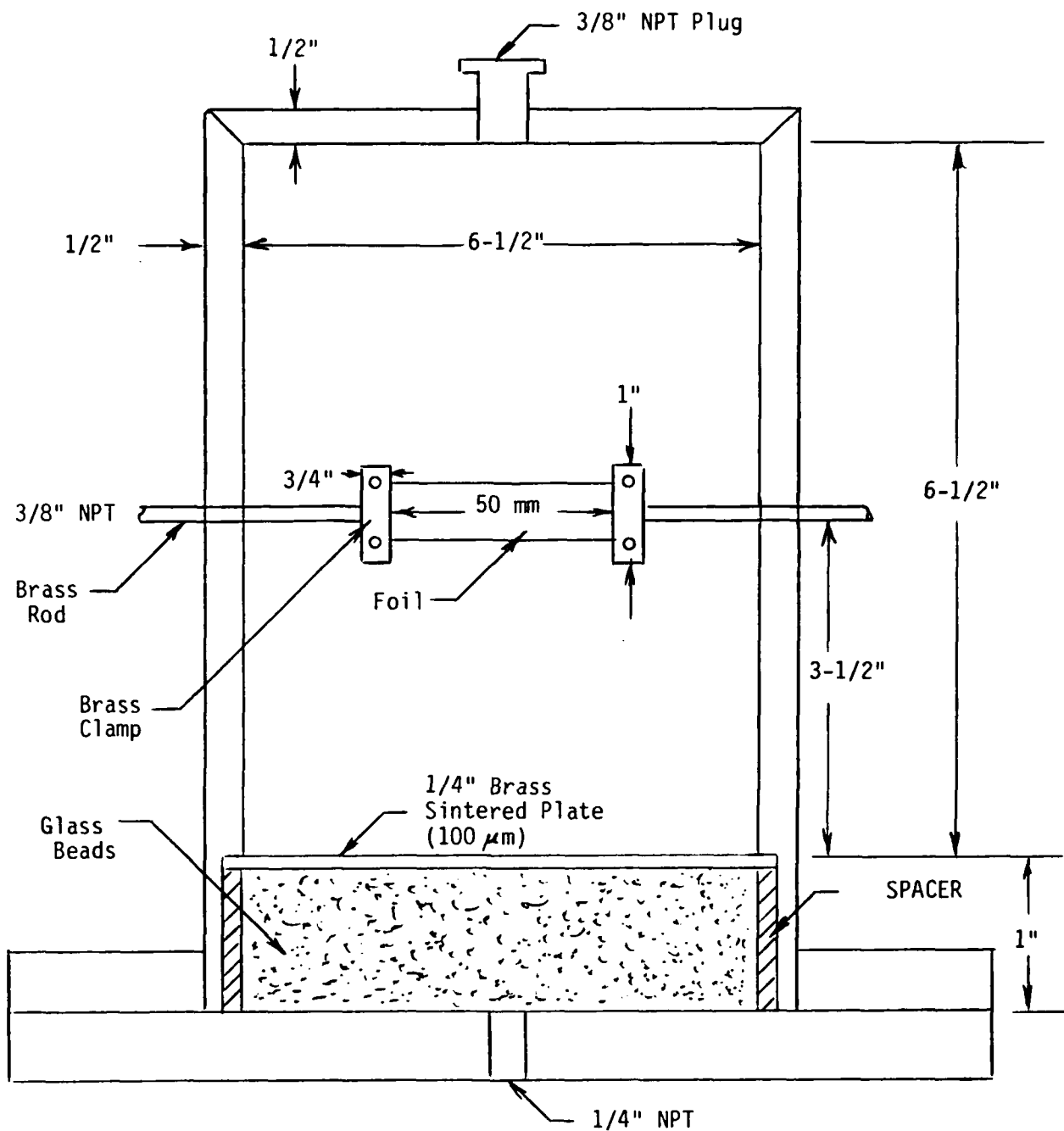
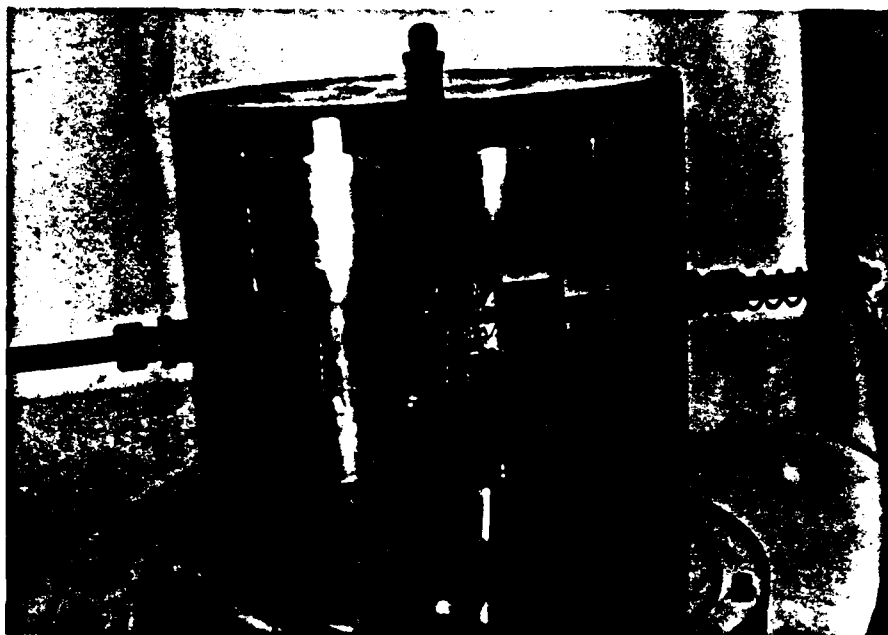


Figure 6. REACTOR CONFIGURATION FOR VAPORIZED FUEL TESTS



- Background: Thermocouple probe for measuring internal ambient temperature.
- Foreground: Phototransistor assembly used for optically monitoring foil surface temperature.

Figure 7. CLOSEUP VIEW OF TEST REACTOR

removed and the opening was enlarged to provide access for injecting liquid fuel in the desired form.

As shown in Figures 6 and 7, the foil to be heated is clamped between two brass electrodes entering through the sides of the reactor and centered approximately 3.5 inches from the top. These had the capability of being rotated to achieve different foil orientations. The right-hand electrode is connected to a spring assembly which could be adjusted to provide the desired amount of tension. This approach allowed the foil to expand freely so as to prevent it from buckling when heated. The mixture temperature inside the reactor prior to the start of each test was measured using a chromel-Alumel thermocouple (0.004 in. wire diameter, 0.012 in. bead diameter) inserted through the back wall of the reactor. This was approximately centered between the foil and the wall at a height of about 1 inch above the foil. During testing, the time-temperature history of the foil surface was monitored by means of an infrared-sensitive phototransistor installed in an opening in the front wall of the reactor.

3.3 Control of Mixture Composition

3.3.1 Vaporized Fuel and Air

All of the testing was performed under conditions where the mixture in the reactor was essentially stagnant. A small amount of flow was necessary, however, to maintain a slightly positive pressure within the reactor and prevent any ambient air leakage into the system. Because of the low flow rates required, it was impractical to achieve accurate direct metering of the fuel. Consequently, an alternative indirect approach was adopted.

The selected method of preparing the fuel/air mixture consisted of saturating an air stream with fuel vapor and mixing it with a stream of dilution air. The relative proportions of the two streams are adjusted to obtain the desired total flow rate and mixture composition. The saturating chamber, shown in Figures 8 and 9, consists simply of an acrylic tube containing a reservoir of liquid fuel through which the air

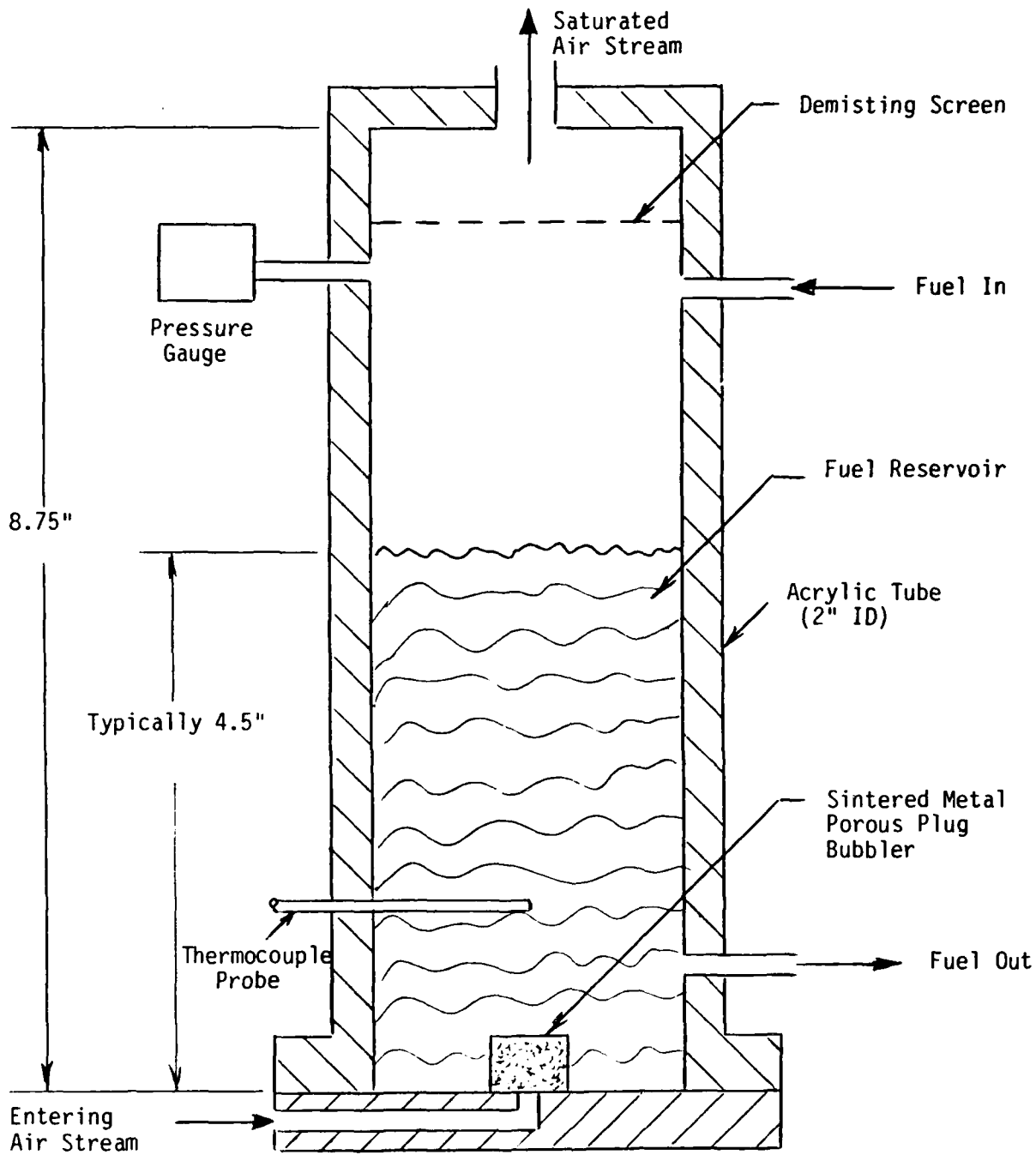


Figure 8. SCHEMATIC OF SATURATING CHAMBER



Overall View



Closeup View

Figure 9. SATURATING CHAMBER USED IN PREPARING VAPORIZED FUEL/AIR MIXTURES

stream to be saturated is bubbled. The temperature of the fuel is adjusted to the desired value and maintained approximately constant by continuously recirculating the fuel through a coil of copper tubing immersed in an insulated 15-gallon tank of water. The same approach is used for controlling the air temperature. The tank was prefilled with water at the required temperature level and provided sufficient thermal storage to maintain satisfactorily constant conditions throughout a given test period.

In order to avoid condensation of the fuel downstream of the saturation chamber, the line carrying the mixed stream to the reactor was heat-traced by coiling the return fuel line around it and wrapping both with insulation. As a further precaution, an electrically-heated coil of Nichrome wire was inserted in the bed of glass beads. This was used to supply a small amount of heating in cases where the fuel/air stream had to be maintained above ambient temperature.

The experimental program was conducted with two different fuels: n-hexane and n-octane. These were procured as reagent-grade chemicals of better than 99 mole % purity. A series of calibration tests was performed with each fuel to examine the operation of the saturating chamber. The tests involved measuring the fuel concentration in the exit air stream as a function of the chamber temperature and pressure. This was accomplished by burning the mixture, measuring the concentration of CO₂ in the resulting combustion products using a Beckman NDIR analyzer, and calculating the corresponding fuel/air ratio in the stream. The results of these tests verified that the chamber operated at essentially 100% efficiency in achieving saturation over a wide range of temperatures and air flow rates.

The procedure followed in filling the reactor with the desired fuel/air mixture consists of two steps. First, the saturated air and dilution air streams are set to give the desired composition and a high total flow rate on the order of 2000 ml/min. The reactor is purged at this rate until at least four volume changes have been obtained. The total flow rate is then reduced rapidly to a low value of around 300 ml/min (selected to keep the velocity in the reactor below 1.5 cm/min) while keeping the same proportion of saturated and dilution air flows. This low

flow rate is maintained constant while conducting the ignition test for the specific mixture composition. Because of the relatively high turndown ratio required between purge and test conditions, two different pairs of rotameters with different flow ranges are used in order to provide sufficient accuracy in setting and measuring the flow rates of the air streams.

3.3.2 Liquid Fuel and Air

For the case of liquid fuel ignition tests, the fuel is sprayed directly into the reactor through a conventional swirl-type pressure atomizer. This is connected to a specially-constructed injection tube fitted with a piston which is activated by high-pressure shop air. The assembly is designed to provide for rapid single-shot injection of a small pre-measured quantity of fuel at high liquid pressures.

The essential design features of the injection tube are given in Figure 10 and photographs of the installation in the reactor are presented in Figure 11. The injector is a machined brass tube with two chambers. The upper one contains a piston fitted with two O-ring seals. The lower chamber serves as a reservoir for liquid fuel. Both the two ports opening into the upper chamber are connected to 3-way solenoid valves. Each of these valves can either supply high-pressure shop air to the chamber or vent it to atmosphere depending on the valve position. The port in the lower chamber is connected through a manual shutoff valve to a pressurized container of liquid fuel. In order to fill the tube, the manual valve is opened, Port #1 is vented to atmosphere, and Port #2 is pressurized. This causes the piston to retract, drawing fuel into the reservoir. In order to inject fuel, the manual shutoff valve is closed, Port #2 is vented, and Port #1 is exposed to high-pressure shop air. This causes the piston to move rapidly downward, forcing fuel through the atomizer at high pressure. The quantity of fuel injected is equal to the displacement volume of the piston in the lower chamber and is adjustable by means of the piston positioning screw.

The injection tube is designed so that any one of a variety of different conventional pressure atomizers can be attached to it. In the current experimental investigation, two atomizers with nominal flow

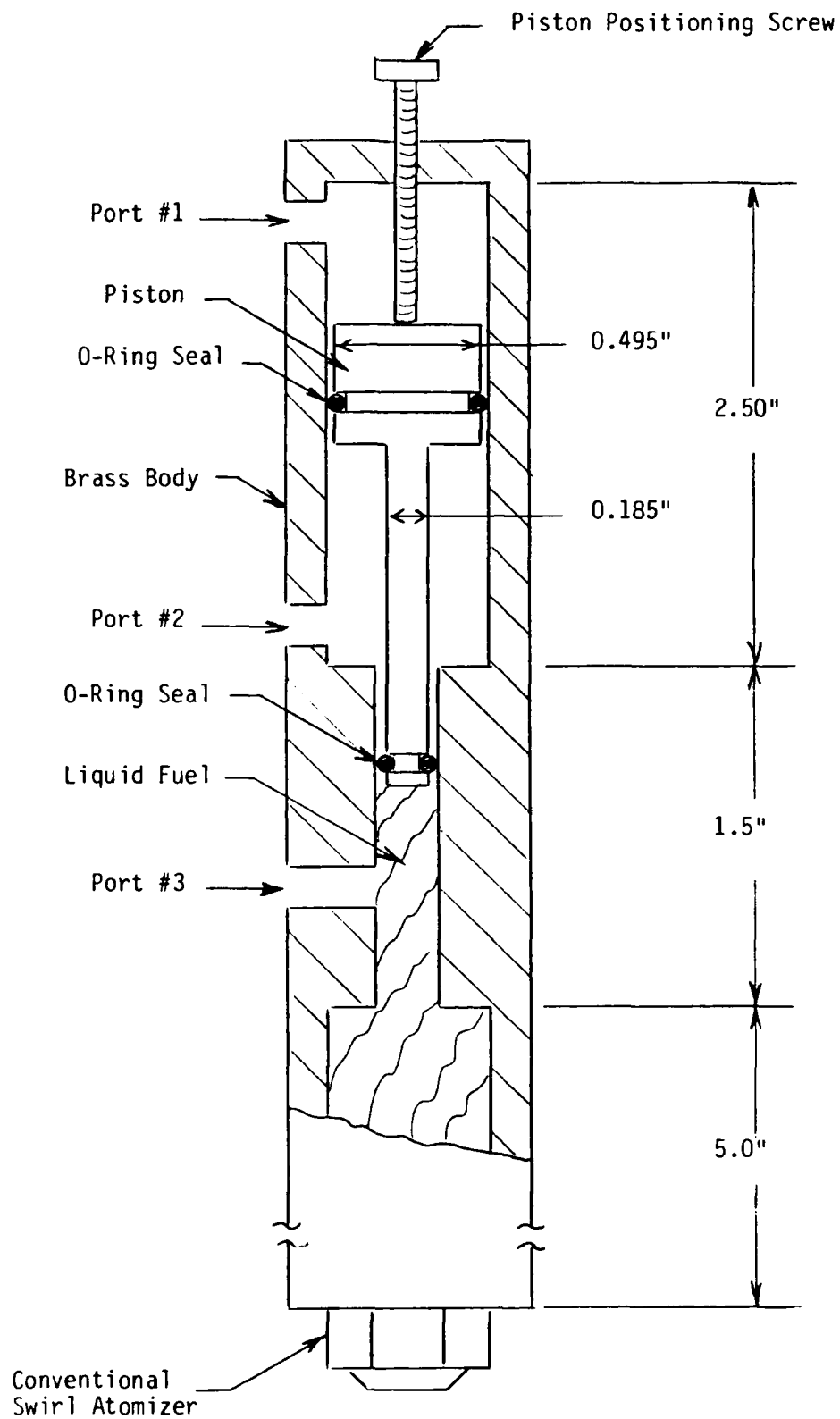
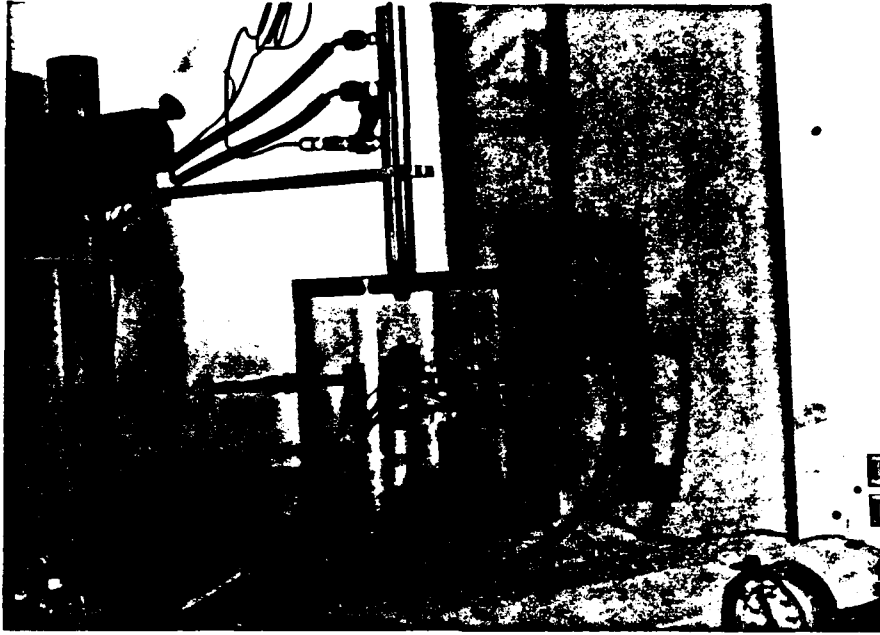


Figure 10. SCHEMATIC OF LIQUID FUEL INJECTION TUBE



Overall View



Closeup View

Figure 11. LIQUID FUEL INJECTION ASSEMBLY

capacities of 0.6 GPH and 2.75 GPH were tested. Both atomizers were conventional oil-burner nozzles supplied by Danfoss Inc. The particular models chosen were swirl-type pressure atomizers producing a solid-cone spray with an 80° spray cone angle. The spray characteristics of the two nozzles are then essentially identical except for mean drop diameter which increases with increasing capacity.

3.4 Heating Circuit

The electrical system used to provide resistance heating of the foil consists of two separate circuits which can be operated independently or in parallel. The overall system is shown schematically in Figure 12. The purpose of the pulse circuit is to achieve rapid initial heating of the foil to the desired temperature. This is accomplished by a bank of six capacitors which are charged to a predetermined voltage and then discharged through the foil. The function of the hold circuit is to maintain the foil temperature constant at the desired value for an indefinite length of time. This requires a circuit which maintains voltage constant at a preset adjustable value. The heating sequence is initiated by setting the pulse and hold voltages to the desired values and then throwing the manual switch which activates both circuits simultaneously.

The ignition tests were conducted with different foils all fabricated from 4.75 mm x 0.10 mm (3/16" x 0.004") Nichrome ribbon material. The general mounting arrangement is shown in Figure 13 for the three different sizes of foil tested. The configuration was essentially identical in all cases except that the largest foil width (L = 9.52 mm) was obtained by butting together two sandwiches of the Nichrome stock material.

The heating circuit was calibrated with each foil in air to determine the combinations of pulse and hold voltages required to obtain different temperature levels. A typical heating curve is shown in Figure 14 for the 4.75 mm foil. As can be seen, the pulse circuit operating alone produces a rapid rise in temperature followed by a gradual decrease with time as the foil loses heat to ambient in the reactor. The combined effect of the

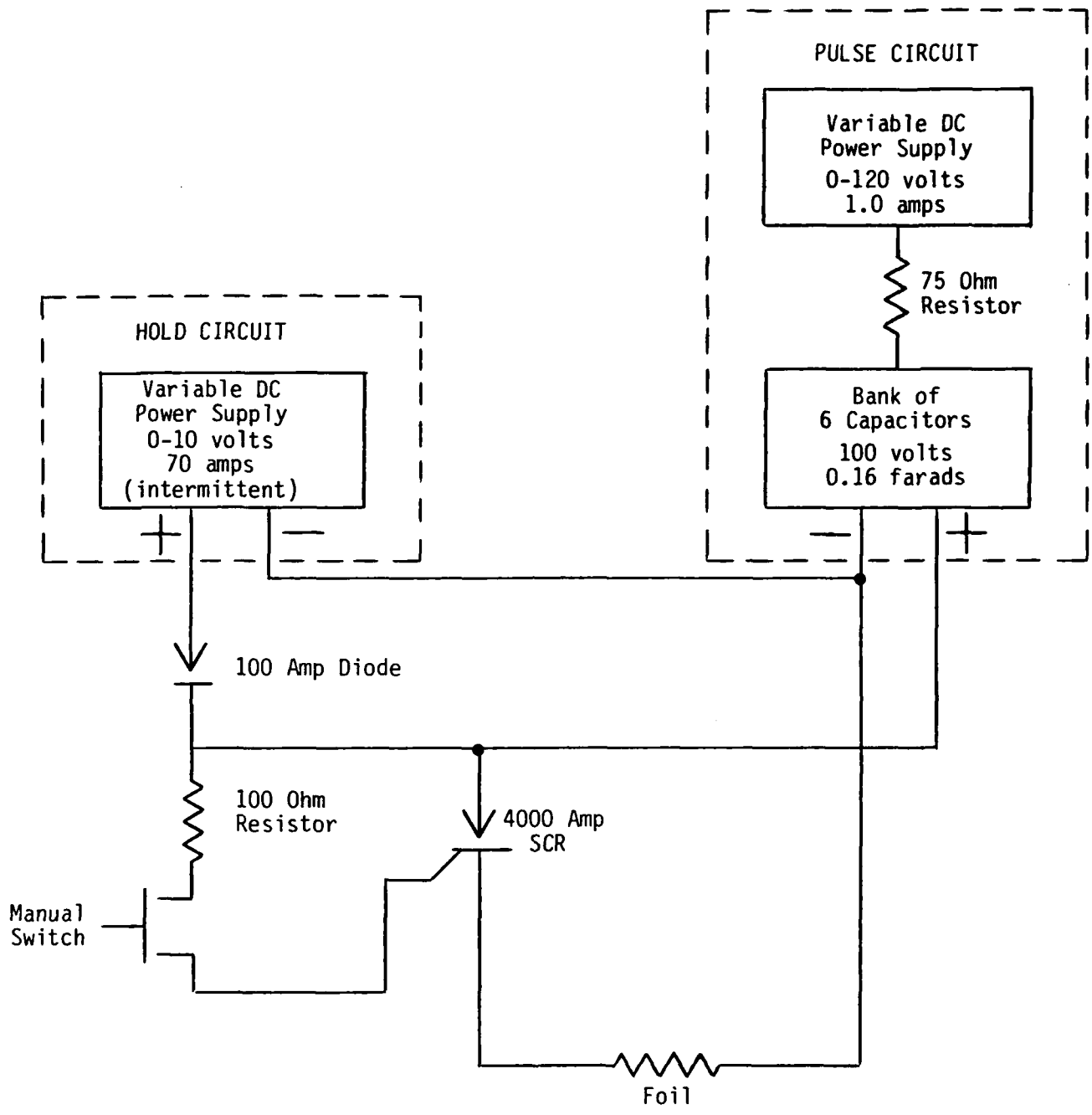
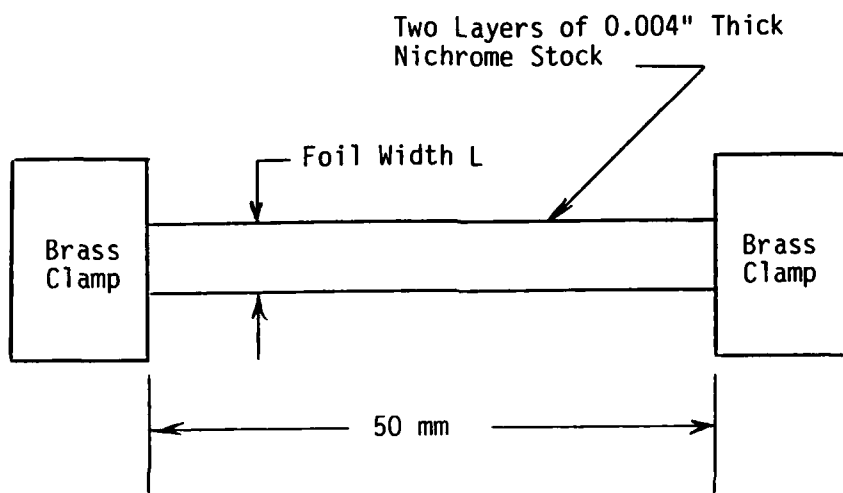


Figure 12. SCHEMATIC OF FOIL HEATING CIRCUIT



Values of
L Tested
mm

2.38	(3/32")
4.76	(3/16")
9.52	(3/8")

Figure 13. FOIL MOUNTING ARRANGEMENT IN REACTOR

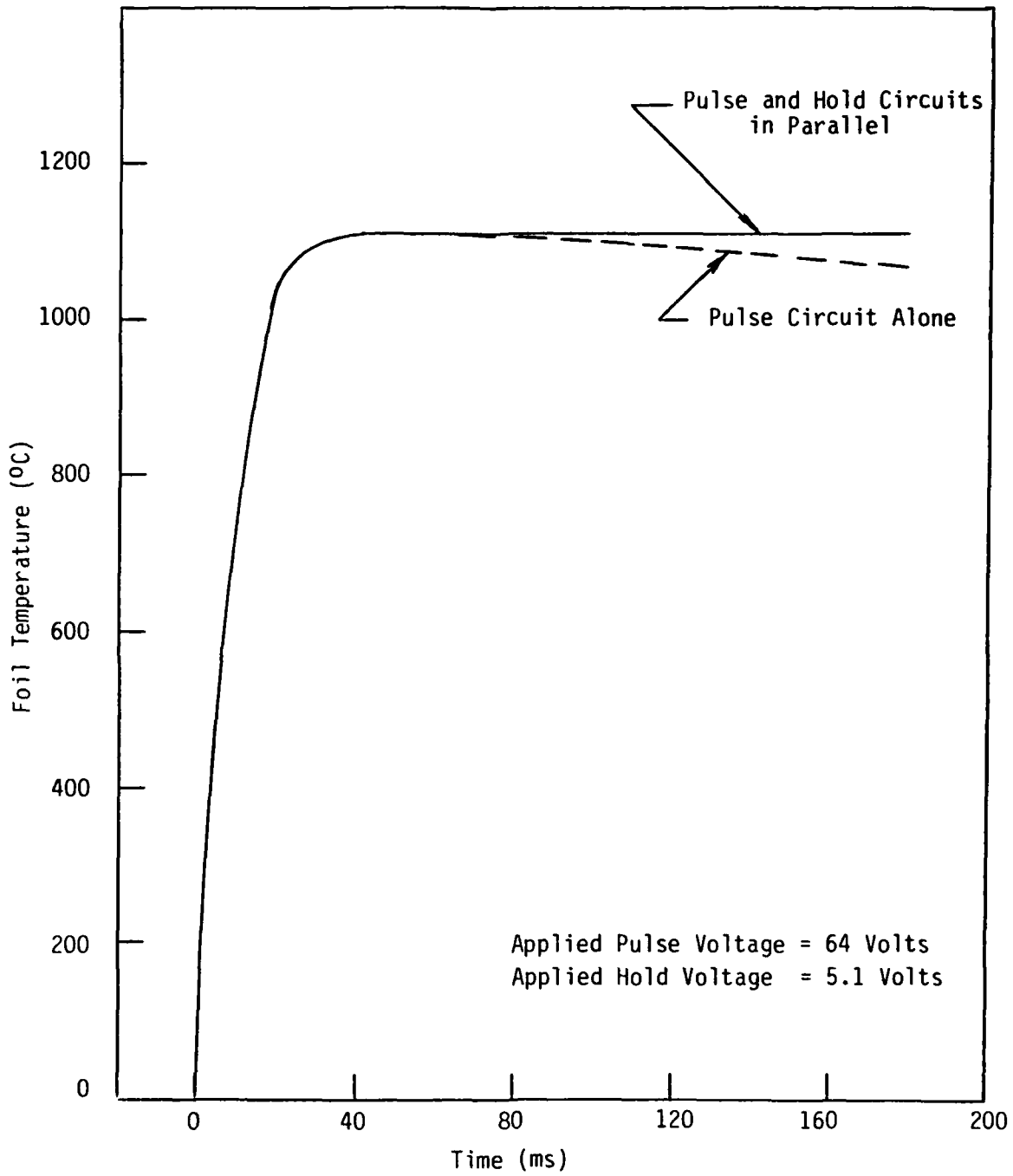


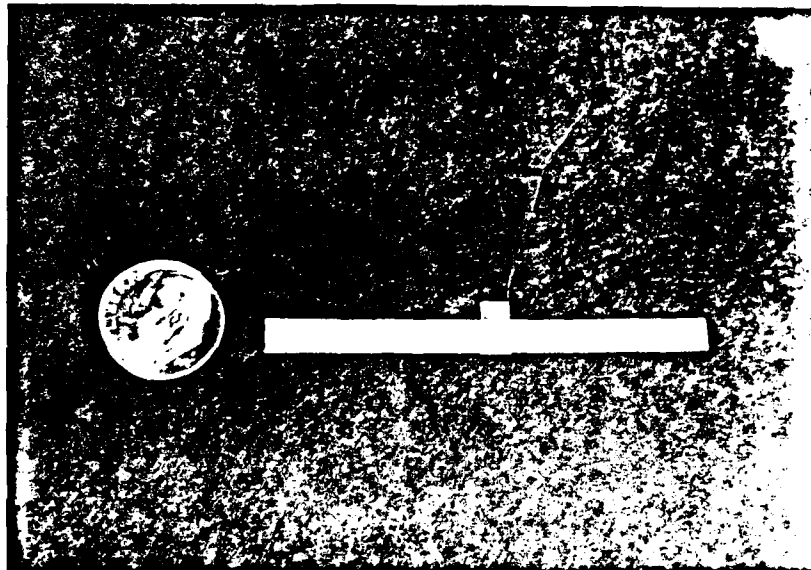
Figure 14. TYPICAL TIME-TEMPERATURE HISTORY FOR 4.76 mm FOIL IN AIR

two circuits operating simultaneously is a temperature curve which rises sharply to the desired level in around 50 ms and remains constant indefinitely as the continuous resistance heating provided counterbalances the heat loss. The corresponding results obtained for other foils and temperature levels exhibited the same characteristics and demonstrated that the selected approach performs quite well in terms of both initial heating time and foil temperature stability.

3.5 Foil Temperature Measurement

The method originally planned for measuring the transient temperature consisted of using fast-response thermocouples between the two foil layers. Preliminary results, however, showed that this was impractical for conducting a large number of tests. The small diameter thermocouple wire required to provide fast response was found to be too fragile to survive more than one ignition. Consequently, an alternative optical technique was developed using an NPN Planar Silicon Phototransistor (General Electric L14G1) selected for sensitivity to infrared radiation. The phototransistor is mounted in an opening in the reactor wall (as shown in Figure 7) and aligned so that the foil is centered in the viewing angle.

Prior to ignition testing of each foil, an in-place calibration was conducted to determine the variation of phototransistor output versus temperature. A small-diameter Chromel-Alumel thermocouple (0.001" wire diameter, 0.003" bead diameter) was sandwiched between two pieces of 0.004" thick mica and inserted between the two Nichrome layers of foil. This assembly is shown in the photograph given in Figure 15 for the 4.76 mm foil. The calibration procedure consisted of electrically heating the foil to a constant temperature and measuring both the thermocouple and phototransistor outputs. The results obtained for three different foils are shown in Figure 16. As can be seen, the phototransistor output is an extremely sensitive measure of surface temperature varying exponentially over the range of interest. Additional confidence in the calibration results is provided by the fact that the phototransistor output is roughly linear with foil width which is what would be expected with perfect alignment.



4.76 mm Foil Assembly

Figure 15. TYPICAL FOIL/THERMOCOUPLE ASSEMBLY FOR
CALIBRATION OF OPTICAL TEMPERATURE
MEASUREMENT TECHNIQUE

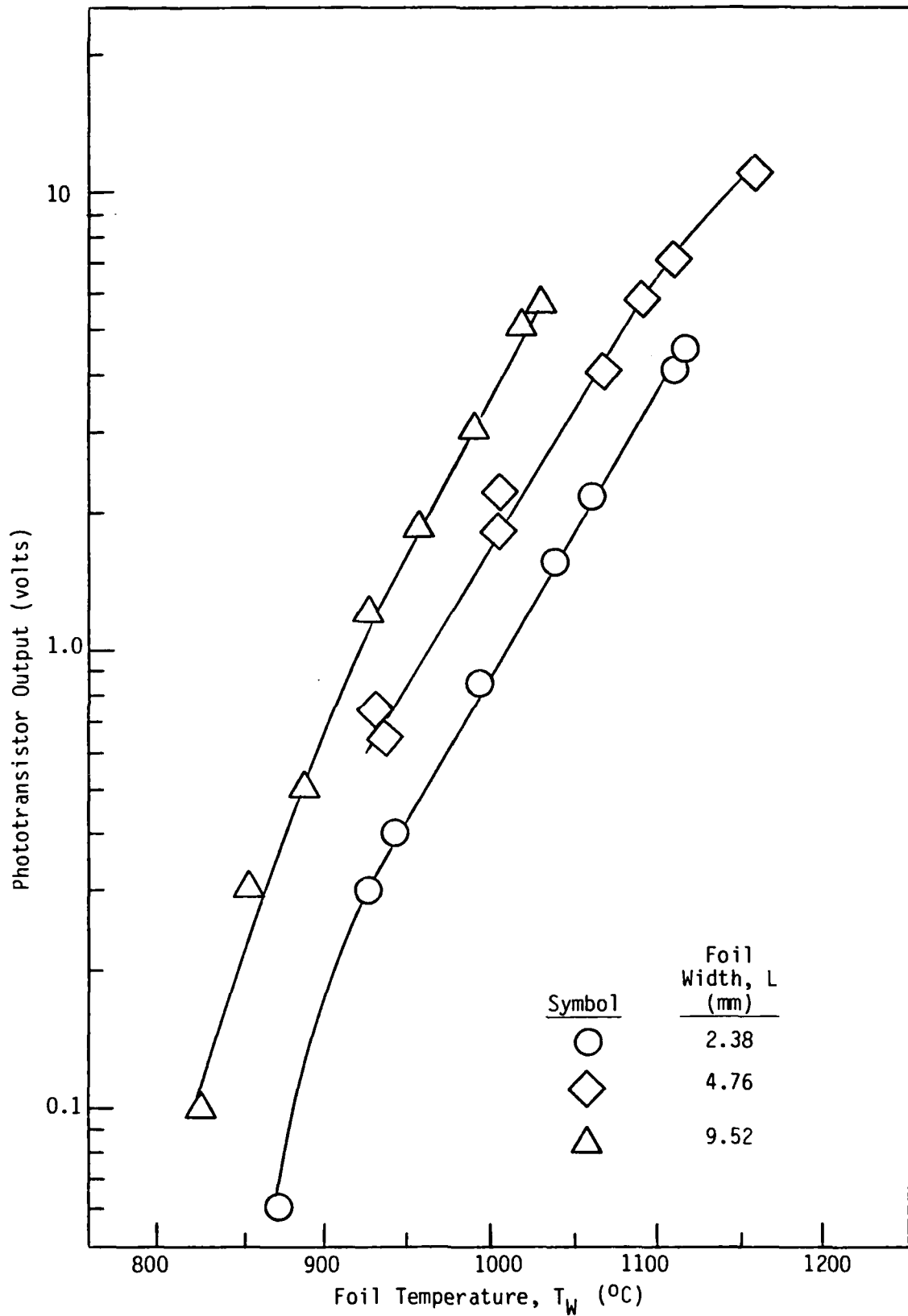


Figure 16. CALIBRATION OF PHOTO-OPTICAL TEMPERATURE MEASUREMENT TECHNIQUE

In conducting subsequent ignition tests with a calibrated foil, the time-temperature history was monitored by storing the transient output from the phototransistor in a Tektronik 5223 Digitizing Storage Oscilloscope. The information was then immediately processed using a Plotmatic 715 X-Y plotter to obtain a hard-copy record of the temperature (voltage) versus time trace. The oscilloscope had the added capability of expanding both scales by a factor of 10, if desired, without losing the stored information. This feature was useful in focusing on specific regions of the curve to examine in detail transient phenomena of interest in certain tests.

The selected optical technique proved to be extremely effective in conducting the ignition tests. One of its main advantages is that it responds essentially instantaneously, eliminating the uncertainty associated with thermocouple time lag. Another advantage is its sensitivity which allows observation of relatively small changes in temperature that can be important in interpreting the ignition process. The only disadvantage is the lower limit on temperature which can be accurately monitored. Fortunately, this was not a drawback in the current study and could easily be eliminated as a potential problem in future work at the expense of a somewhat more complicated design.

3.6 Test Procedures

3.6.1 Vaporized Fuel Ignition Tests

Each test for a given foil is initiated by purging the reactor with the selected fuel/air mixture and then reducing the flow rate to the required test value. The ambient temperature within the reactor is recorded. The heating circuit voltages are set to the values required to give a foil temperature below what is expected for ignition. The heating circuit is activated maintaining the foil temperature constant for a predetermined length of time typically around 5 sec. During this interval the time-temperature history of the foil is stored on the oscilloscope and subsequently plotted using the X-Y plotter. If ignition does not occur, the foil and reactor are allowed to cool down to the starting conditions. A new set of voltages is selected to obtain a higher foil temperature (nominally 30°C above the previous value) and the cycle is repeated. This

process is continued, incrementing the temperature in each trial, until ignition occurs. The flow is then turned off and the reactor is purged with pure air. Without changing the heating circuit voltage settings, the foil is again heated in air and the time-temperature history is recorded providing a comparison with the corresponding ignition trace.

For purposes of illustration, the results obtained in a typical test are presented in Figure 17. In this case, three different foil temperatures were investigated. Ignition occurred for a foil temperature of 960°C (1760°F) with a delay time of approximately 400 ms. The onset of ignition is readily apparent as the point at which the temperature rises sharply in comparison to the corresponding flat profile in air. When ignition occurs the reactor cover rises and allows ambient air to rush in producing the observed decrease in temperature after combustion has been completed. As demonstrated by these test results, the selected experimental procedure is an extremely effective method of obtaining detailed data on the thermal ignition process.

3.6.2 Liquid Fuel Ignition Tests

The procedure followed in the case of liquid fuels differs in some respects from that described above for vaporized fuel/air mixtures. Each test consists of examining the ignition process for a given foil at one temperature level. Prior to starting a test, the ambient air temperature within the reactor is recorded and the heating circuit voltages are set to the values required to achieve the desired foil temperature above what is expected for ignition. The heating circuit is activated and the temperature is held constant for a given length of time. The pre-determined quantity of liquid fuel is then sprayed rapidly into the reactor. This is accomplished by activating the solenoid valve which pressurizes the piston contained in the injection tube. The time-temperature history is recorded starting at the point when the injection is initiated. The foil heating is continued for approximately 5 sec. When ignition occurs, the injected fuel is allowed to burn out and the reactor is flushed completely with air in preparation for the next test at a lower temperature. The testing of a given foil is continued until a temperature is reached where no ignition occurs.

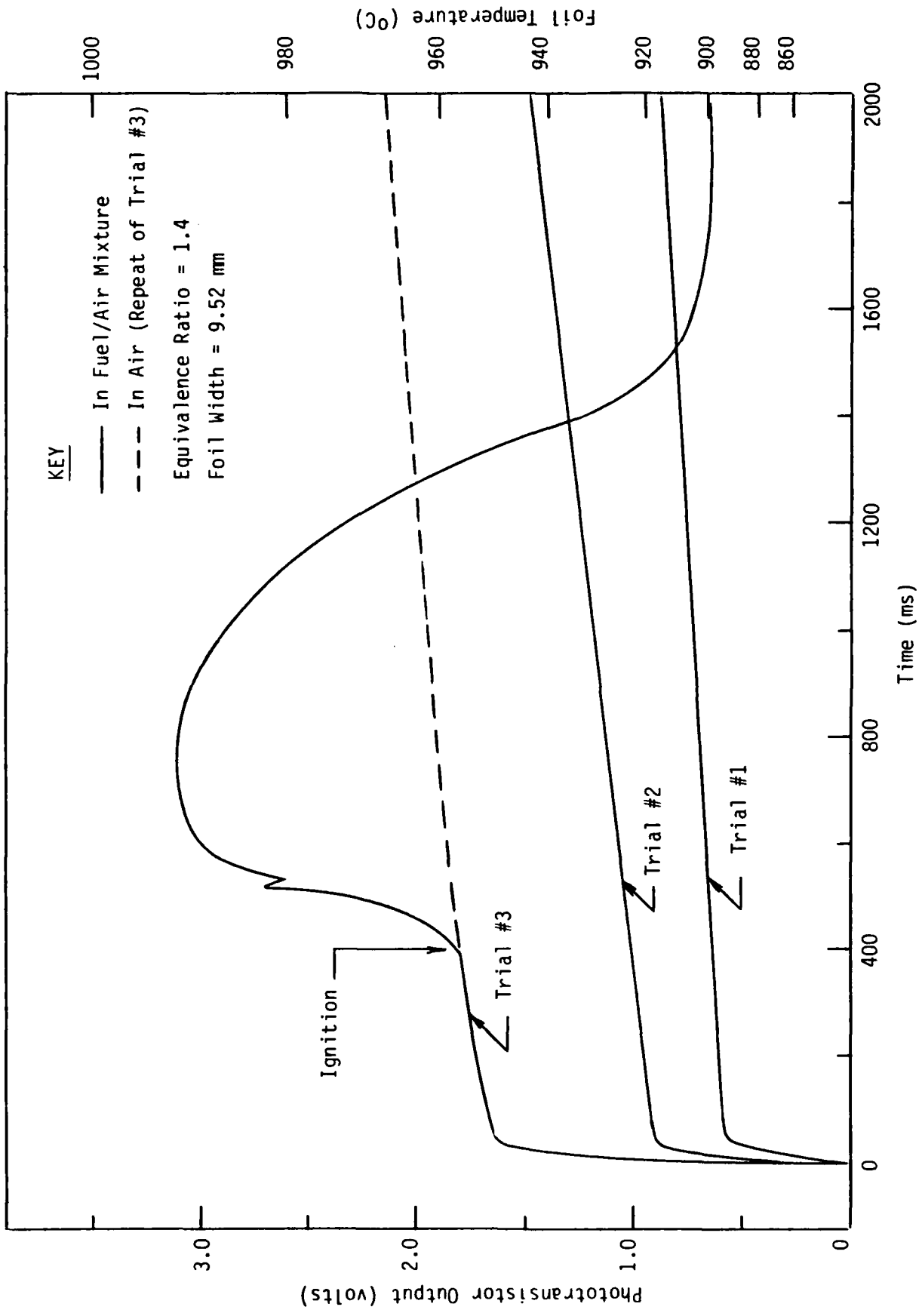


Figure 17. TYPICAL TEST RESULTS FOR VAPORIZED HEXANE/AIR MIXTURE

Figure 18 shows the recorded time-temperature history obtained in a typical test. Following the start of the injection process, the foil temperature remains constant for about 450 ms until the spray reaches the foil. At this point in time, the increased heat loss due to the presence of the liquid phase results in a slight but obvious decrease in temperature which is observable because of the sensitivity of the optical measurement technique. The gradual cooling of the foil continues until ignition occurs resulting in a sudden increase in temperature. As indicated in Figure 18, the ignition delay time, which is about 150 ms in this case, is determined approximately by measuring the interval between the start of cooling and the onset of ignition.

The optical technique provides an effective means of monitoring the foil temperature variation even in the presence of a spray. This is because liquid sprays of the type investigated are essentially transparent to radiation in the infrared portion of the spectrum. In any event, the phototransistor is aligned with the foil. Consequently, the phototransistor output would still provide an accurate indication of when the spray reaches the foil even if the observed decrease were partially due to obscuration.

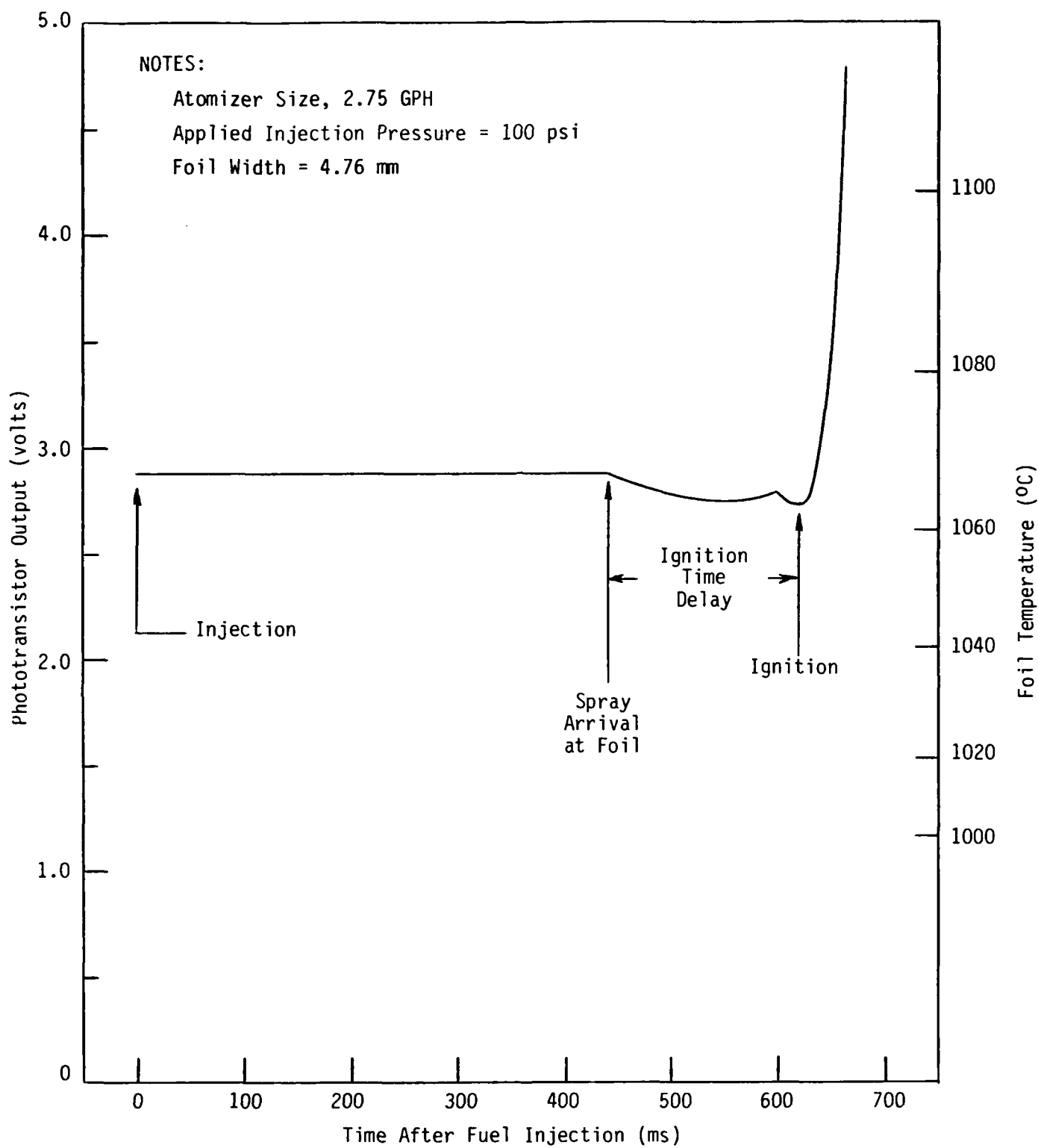


Figure 18. TYPICAL TEST RESULTS FOR OCTANE LIQUID SPRAY IGNITION

4. ANALYSIS AND CORRELATION OF TEST RESULTS

4.1 Parametric Experimental Investigation

An initial set of preliminary tests was conducted for the purpose of debugging the apparatus, establishing an effective test protocol, and determining the appropriate ranges of conditions to be examined. Two separate series of detailed parametric tests were then performed to determine the ignition temperature and delay time for various conditions. In all, a total of over 120 tests were conducted.

The first series of parametric tests investigated the ignition process for mixtures of vaporized fuel and air. The pertinent results obtained are summarized in Table 1. Most of the testing was done with hexane because the high volatility of this fuel made it simple to prepare vapor mixtures at temperatures close to ambient. A number of tests were also done with octane to provide a benchmark against which to compare the results of subsequent liquid testing where low volatility was required. As shown in Table 1, the series of vaporized fuel tests covered the following ranges of the major parameters:

Foil Width	2.38, 4.76, 9.52 mm
Equivalence Ratio	0.4-2.2
Surface Temperature	870-1120°C
Duration at Temperature	2-10 sec

The second series of ignition tests was conducted with sprays of liquid octane. As mentioned above, this fuel was selected because its volatility was low enough to insure that a negligible amount of vaporization would occur at ambient temperature within the reactor eliminating this factor as a potential source of error. The quantity of fuel injected in each test was equivalent to the value which would produce a stoichiometric concentration if mixed with the total volume of air in the reactor. The actual fuel/air ratio in the vicinity of the foil was, of course, greater than stoichiometric during the injection process.

Table 1

SUMMARY OF EXPERIMENTAL IGNITION RESULTS FOR MIXTURES OF VAPORIZED FUEL AND AIR

Test No.	Fuel	Foil Width, L (mm)	Nominal Equivalence Ratio ϕ	NO IGNITION(1)			IGNITION		
				Duration at Temperature (sec)	Ambient Reactor Temperature T_e (°C)	Foil Temperature T_w (°C)	Ambient Reactor Temperature T_e (°C)	Foil Temperature T_w (°C)	Delay Time τ_R (ms)(2)
1	n-Hexane	2.38	0.6	5	19	960	20	1000	120
2	n-Hexane	2.38	0.7	5	20	970	21	1000	90
3	n-Hexane	2.38	0.8	5	21	970	21	1010	1200
4	n-Hexane	2.38	1.0	5	20	970	21	995	3200
5	n-Hexane	2.38	1.0	5	20	940	21	1000	3500
6	n-Hexane	2.38	1.0	5	18	985	18	1015	0+
7	n-Hexane	2.38	1.0	2	--	---	22	1025	0+
8	n-Hexane	2.38	1.0	10	19	970	20	1035	0+
9	n-Hexane	2.38	1.0	5	--	---	20	1055	0+
10	n-Hexane	2.38	1.2	5	20	970	20	1010	800
11	n-Hexane	2.38	1.4	5	21	925	22	1010	3000
12	n-Hexane	2.38	1.8	5	21	985	21	1035	4500
13	n-Hexane	2.38	2.0	5	19	1000	19	1045	1700
14	n-Hexane	4.76	0.6	5	22	915	22	975	0+
15	n-Hexane	4.76	0.8	5	24	955	24	985	0+
16	n-Hexane	4.76	1.0	10	22	940	23	971	0+
17	n-Hexane	4.76	1.0	5	20	940	21	985	500
18	n-Hexane	4.76	1.2	5	21	945	22	990	0+
19	n-Hexane	4.76	1.4	5	24	985	25	1020	0+
20	n-Hexane	4.76	1.8	5	25	995	25	1020	0+
21	n-Hexane	4.76	2.0	5	26	995	26	1025	0+
22	n-Hexane	9.52	1.0	5	24	870	24	895	4600
23	n-Hexane	9.52	1.0	5	--	---	23	925	1500
24	n-Hexane	9.52	1.0	5	25	920	24	950	2800
25	n-Hexane	9.52	1.0	2	--	---	24	1010	0+
26	n-Hexane	9.52	1.2	5	22	900	22	935	900
27	n-Hexane	9.52	1.4	5	--	---	23	950	0+
28	n-Hexane	9.52	1.4	2	23	925	23	960	400
29	n-Hexane	9.52	1.8	2	22	885	22	925	1760
30	n-Hexane	9.52	1.8	5	--	---	22	945	1900
31	n-Hexane	9.52	1.8	2	22	925	22	960	350
32	n-Hexane	9.52	1.8	5	25	935	21	970	500
33	n-Hexane	9.52	2.0	2	22	925	22	955	0+
34	n-Hexane	9.52	2.0	5	23	925	23	955	700
35	n-Hexane	9.52	2.0	5	21	950	21	990	0+
36	n-Octane	4.76	0.4	5	28	1120	--	---	---
37	n-Octane	4.76	0.6	5	27	955	27	990	0+
38	n-Octane	4.76	0.8	5	28	925	28	960	0+
39	n-Octane	4.76	1.0	5	29	925	29	960	0+
40	n-Octane	4.76	1.1	5	30	925	30	960	0+
41	n-Octane	4.76	1.4	5	23	940	25	970	0+
42	n-Octane	4.76	1.6	5	28	960	29	990	0+
43	n-Octane	4.76	1.9	5	30	960	29	990	0+
44	n-Octane	4.76	2.2	5	27	925	27	990	0+

- NOTES: 1. For a given test, these values correspond to the highest foil temperature tried for which no ignition occurred.
 2. A value of 0+ in this column indicates that ignition occurred within the initial foil heatup time which was typically less than 50 ms.

Fortunately, as will be shown subsequently, the thermal ignition process appears to be relatively insensitive to concentration. The effect of mean drop size was examined by varying injection pressure and testing sprays from two atomizers differing only in flow capacity. All testing was performed with a 4.76 mm wide foil heated to different temperature levels over the range 890-1090°C.

4.2 Correlating Equations

The analytical model derived in a previous section of this report results in a number of expressions for predicting the components of the overall ignition delay time. A steady-state version of the model also provides an expression for the critical hot-surface dimension required for ignition. Different forms of the expressions are obtained depending on the prevailing mode of heat transfer. In all cases, however, the analytical equations are functions of known quantities, such as fuel properties, ambient conditions, and geometry. They also contain several parameters related to the reaction chemistry which have physical significance, but whose values are not known precisely. These consist of the reaction orders with respect to fuel and oxidizer (m_F and m_O), the frequency factor (A), and the activation energy (E).

The analytical model has been applied in correlating the test data. In preparation for describing the detailed results obtained it is useful to present the simplified forms of the correlating equations which were found to be appropriate to the ranges of test conditions investigated. In this regard, the first simplification consisted of determining the specific mode of heat transfer prevailing in the test configuration. As would be expected, the results demonstrated quite clearly that natural convection was the predominant mechanism for heat transfer from the heated foil. This observation is confirmed by the results obtained by Laurendeau and Caron (Ref. 2) with essentially the same geometry.

For most hydrocarbons, the overall reaction order is around 2. A reasonable simplifying approximation is to assume that $m_F = 1$ and $m_O = 1$. Although the precise value of the activation energy is uncertain, available data on similar hydrocarbons (Ref. 1) would indicate that E/R

should be on the order of 20,000°K. This provides some guidance in determining the appropriate range of values to be examined. The greatest degree of uncertainty lies in assigning a value to the frequency factor, A. In correlating the test results, therefore, this parameter has been treated as the principal empirical constant whose value is adjusted as necessary to calibrate the analytical model. Although this approach is not strictly correct in a theoretical sense, it was found to be quite useful in producing practical correlations of the experimental data.

4.2.1 Correlating Equation for Ignition Temperature

In analyzing the test data it was found that the ignition conditions were relatively insensitive to equivalence ratio. The predicted effect of equivalence ratio assuming constant values of the reaction chemistry parameters (m_f , m_o , E, and A) did not, however, quite match the observed effect. This is not too surprising, since one would intuitively expect these parameters to be somewhat dependent on mixture composition. From a practical standpoint the most expedient method of accounting for this minor dependency was to apply a small empirical correction factor to the expression relating characteristic surface width to ignition temperature, fuel properties, and mixture composition. Assuming natural convection and a second-order reaction results in the following final form of the correlating equation:

$$L = \left(\frac{C_{NC}}{k}\right)^4 \left(\frac{E^* B_1 f_p}{A}\right)^2 f_T (T_e \theta_w)^3 \exp\left(\frac{2E^*}{\theta_c}\right) \quad (48)$$

where $C_{NC} = 4.33 \times 10^{-4} \text{ J/sec-cm}^{1.75} - (\text{OK})^{1.25}$ and B_1 , f_p , f_T are variable groupings defined as:

$$B_1 = \frac{\alpha C_p}{2Q\rho_e Z} \quad (49)$$

$$f_p = \frac{(1+Z\theta)^2}{\theta} \quad (50)$$

$$f_T = \frac{\theta_w - 1}{\theta_w} \quad (51)$$

In obtaining these equations, the fuel and oxidizer concentrations have been expressed in terms of equivalence ratio (θ):

$$\theta = \frac{X_F/X_O}{Z} \quad (52)$$

where Z is the stoichiometric fuel/air ratio on a molar basis. The term θ_C contains the empirical correction factor and is defined as:

$$\frac{1}{\theta_C} = \frac{1}{\theta_W} + C_E (\theta - 1) \quad (53)$$

where C_E is an empirical constant found to be approximately 0.017.

4.2.2 Correlating Equations for Ignition Delay Time

The transient model resulted in separate expressions for the contributions of vaporization, mixing, and reaction to the total ignition delay time. For natural convection and a second-order reaction, the equation for the reaction time becomes:

$$\tau_R = \frac{1}{\pi\alpha} \left(\frac{C_{NC}}{k} \right)^4 \left(\frac{E^* B_1 f p}{A} \right)^{2.5} f_T^6 (T_e \theta_W)^{3.5} \exp(2.5E^*/\theta_W) \quad (54)$$

The corresponding equations for the vaporization and mixing times are as follows:

$$\tau_V = B_2 \left(1 + B_3 G_p \frac{L^{5/4}}{\theta_W^{1/3} (\theta_W - 1)^{1/4} a_0} \right) \frac{a_0^2}{\theta_W - 1} \quad (55)$$

$$\tau_M = B_4 \left(\frac{1 + Z\theta}{\theta^{2/3}} \right) \frac{a_0^2}{\theta_W^{1/3}} \quad (56)$$

where the variable groupings B_2 , B_3 , G_p and B_4 are defined as:

$$B_2 = \frac{\lambda}{4kN_{uD}T_e} \quad (57)$$

$$B_3 = \left(\frac{2\pi N_{uD}}{3C_{NC}T_e^{1/4}} \right) \left(\frac{6\rho_e Z}{\rho_L} \right)^{2/3} \quad (58)$$

$$G_p = \left(\frac{\phi}{1+Z\phi} \right)^{2/3} \quad (59)$$

$$B_4 = \left(\frac{F(C_x)}{6D_V N_{uD}} \right) \left(\frac{\rho_L}{Z\rho_e} \right)^{2/3} \quad (60)$$

and the function $F(C_x)$ is given by Equation 25.

4.3 Ignition of Vaporized Fuel/Air Mixtures

4.3.1 General Observations

Analysis of the thermal ignition process indicates strongly that the most important parameter influencing the ignition conditions is the temperature of the heated surface. This effect is illustrated by the results presented in Figure 19 for three different surface temperatures. At the lowest temperature, ignition was not obtained within the total trial period of 5 sec. Increasing the temperature by about 50°C resulted in ignition approximately 1.5 sec after initiation of foil heating. The final curve shows that ignition occurs almost immediately within the initial heatup period when the temperature level is increased by an additional 80°C. The observed variation in delay time of at least several orders of magnitude provides a convincing demonstration of the sensitivity of the ignition mechanism to temperature.

An interesting phenomenon which sheds some light on the thermal ignition process was observed in a significant number of tests where comparatively long delay times were obtained. This phenomenon is shown in Figure 20 where the temperature profiles in the fuel/air mixture are compared to the corresponding profiles in air for two different temperature levels. The lower pair of curves labeled Trial #1 corresponds to the case where no ignition was obtained within 5 sec. The temperature in the fuel/air mixture, however, is slightly higher than the flat profile

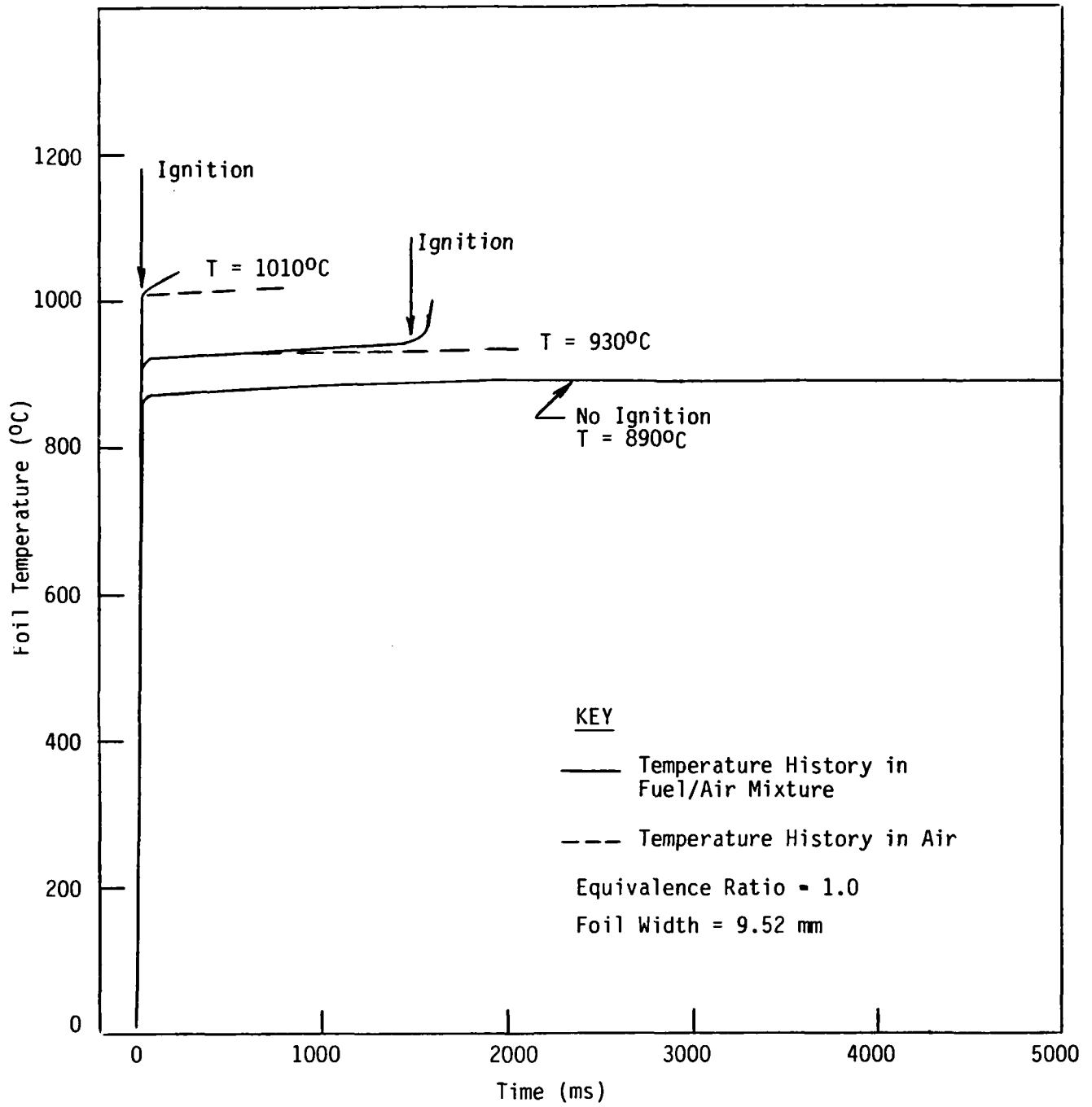


Figure 19. TYPICAL EFFECT OF HOT-SURFACE TEMPERATURE ON IGNITION CONDITION

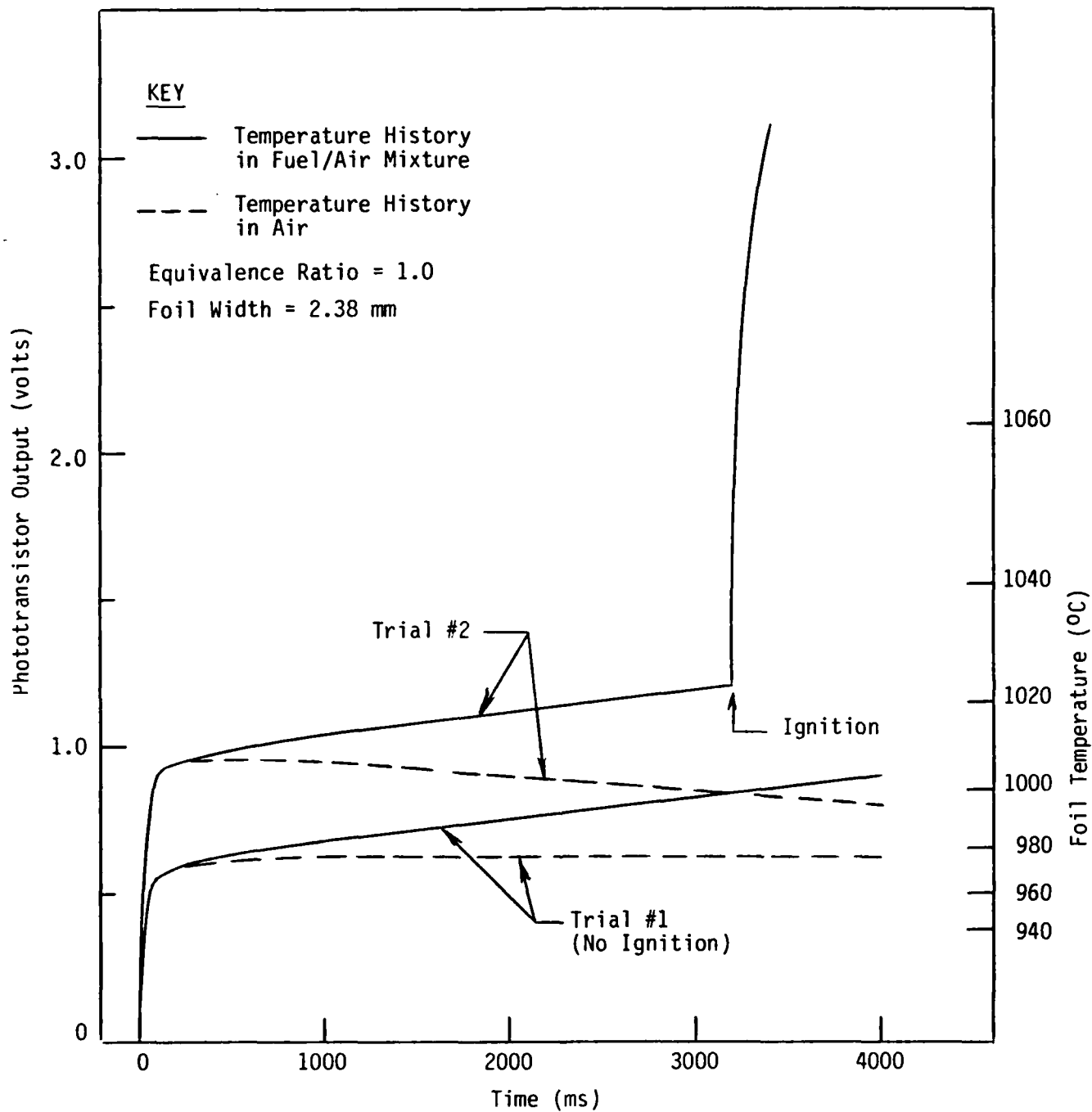


Figure 20. APPARENT EFFECT OF SURFACE REACTION ON PREIGNITION TEMPERATURE PROFILE

obtained in air. The same effect is observed in the upper pair of curves where ignition occurred after about 3.2 sec. These results indicate that the actual ignition event is preceded by a period of comparatively slow chemical reaction in the vicinity of the heated surface. The local mixture temperature then gradually increases until a value is reached where the rate of oxidation rises sharply marking the onset of ignition.

4.3.2 Ignition Temperature

An assumption implicit in the derivation of the steady-state model is that there is a minimum temperature below which ignition cannot be achieved for a given hot-surface size. This is not strictly correct, since the autoignition temperature of a fuel represents a measure of the absolute minimum value which is independent of geometry. For a given surface size then one would expect to find a range of ignition temperatures corresponding to different delay times. This is generally what was observed in the experimental investigation.

Despite the approximation inherent in the steady-state model, it is still a useful analytical tool for correlating the relative effect of geometry on ignition temperature. This is due to the fact that the ignition process is so extremely sensitive to surface temperature. Consequently, as shown previously, the ignition delay time increases dramatically over a comparatively narrow band of temperatures. For all practical purposes then there does exist a minimum temperature below which the delay time is essentially infinite.

The test results obtained in the present investigation provide an approximate measure of the minimum ignition temperature. This, of course, is subject to the limitations on ignition trial time imposed by the scale of the apparatus. The maximum trial time was generally limited to around 5 sec because higher values tended to produce bulk heating of the reactor contents which then violates the basic assumption of an infinite environment. Strictly speaking then the test data should be interpreted as representing the minimum ignition temperature below which the delay time exceeds 5 sec.

For a given set of test conditions, the minimum ignition temperature lies between the highest trial value for which no ignition was obtained and the lowest trial value producing ignition. The data presented in Table 1 provide a measure of this minimum value for hexane and octane as a function of equivalence ratio and hot-surface width.

Examination of Equation 48 suggests that a plot of $\ln(L)$ versus $1/\theta_w$ evaluated at the minimum ignition temperature should produce a family of parallel straight lines corresponding to different constant values of equivalence ratio for a given fuel. The slope of these lines should correspond to the activation energy for the fuel oxidation reaction. Figure 21 shows the test data obtained for hexane plotted in this manner. The two straight lines which bound the data correspond to the predicted variation with the values of A and E adjusted to correlate the test results. As can be seen, except for a few outlying points, the agreement between theory and experiment is quite good and indicates an activation energy of $E/R = 18,000^\circ\text{K}$. By way of comparison, a value of $E/R = 21,000^\circ\text{K}$ was determined by Laurendeau (Ref. 1) for methane. Since one would expect the activation energy to decrease with increasing molecular weight, the empirically determined value appears to be quite reasonable.

The correlation of the hexane data is demonstrated in more familiar terms in Figure 22 where the minimum ignition temperature [corrected to 21°C (70°F) ambient] is plotted versus equivalence ratio for each of the three different foil sizes investigated. The data demonstrate that ignition temperature is surprisingly insensitive to equivalence ratio although a slight minimum is observed at the stoichiometric condition. The curves shown in the figure correspond to the predicted variations. As can be seen, the agreement with the experimentally observed variation is quite good.

Figure 23 presents a comparison of the ignition temperatures determined for the two different fuels tested. In general, the variation with equivalence ratio is the same for both. The principal difference is that the ignition temperature for the heavier hydrocarbon octane is somewhat lower than for hexane. The correlation of the octane data indicates an activation energy equivalent to that determined for hexane,

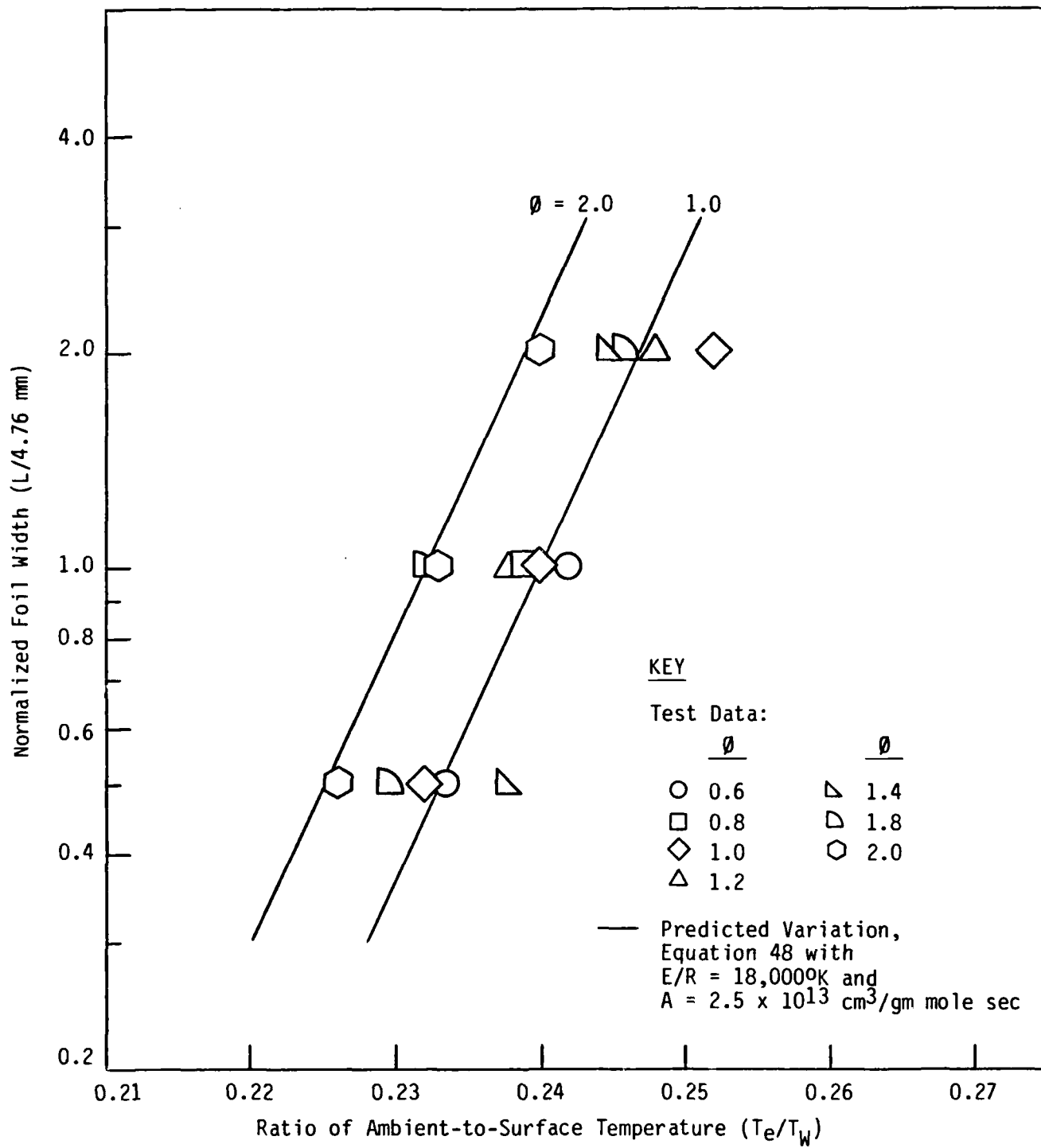


Figure 21. CORRELATION OF IGNITION TEMPERATURE DATA FOR HEXANE VAPOR

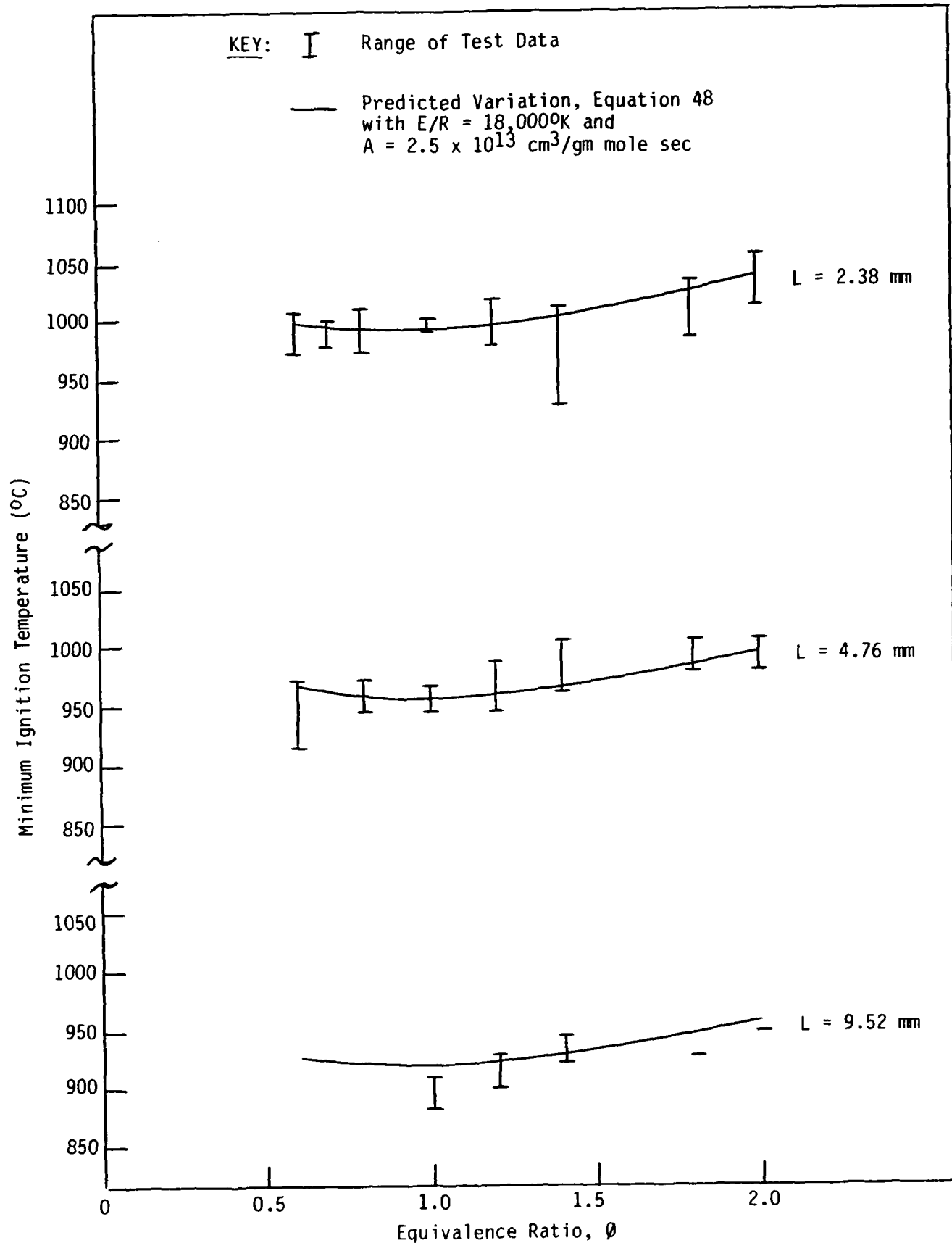


Figure 22. VARIATION OF IGNITION TEMPERATURE WITH EQUIVALENCE RATIO AND FOIL SIZE FOR HEXANE VAPOR

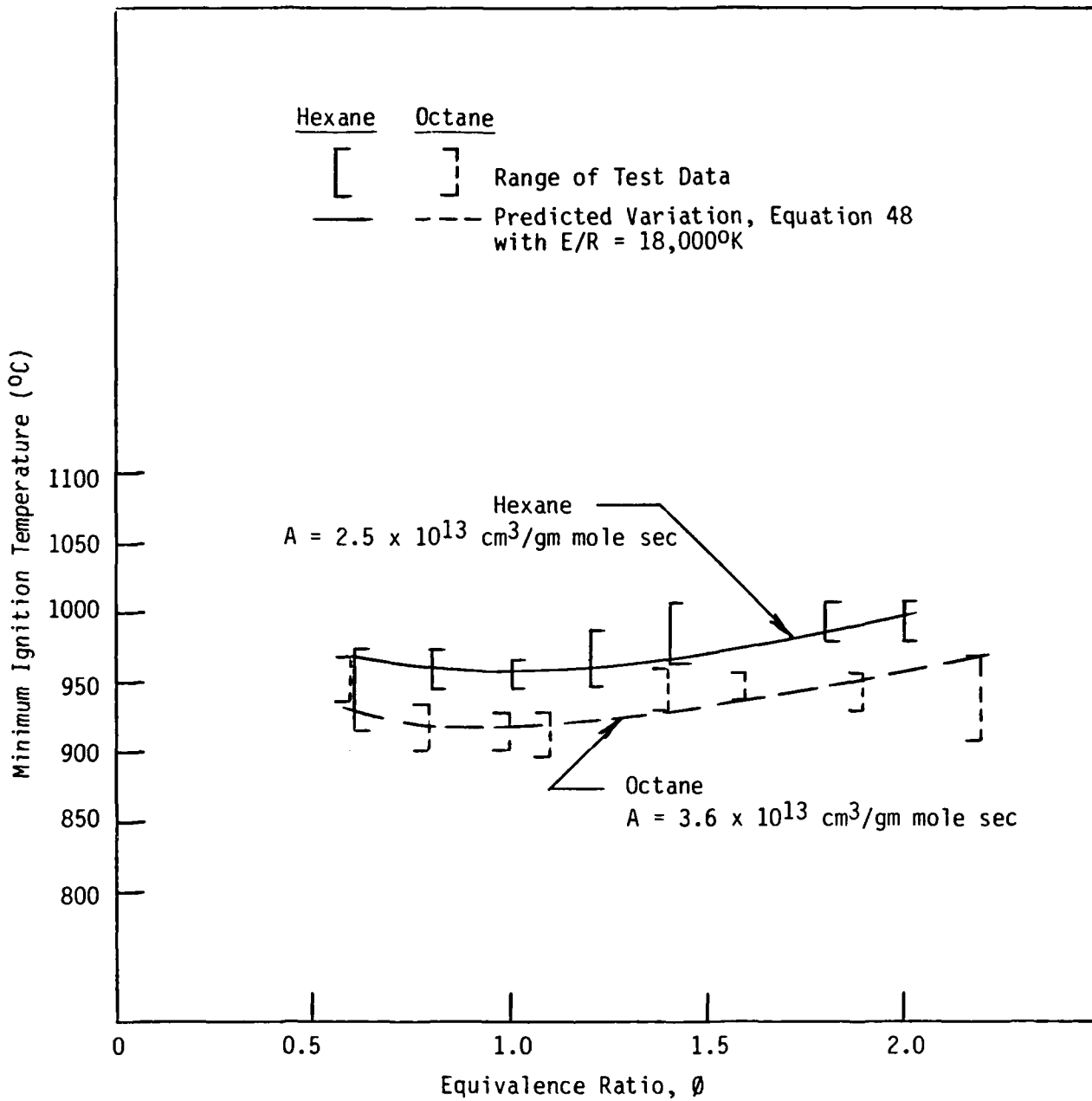


Figure 23. COMPARISON OF IGNITION TEMPERATURE FOR HEXANE AND OCTANE WITH 4.76 mm FOIL

but a slightly higher value of the parameter A. Although the agreement with the experimental results for octane is not quite as good as in the case of hexane, it is still acceptable considering the limited amount of data.

The lowest value of equivalence ratio ($\phi = 0.6$) corresponds approximately to the lean flammability limit for both fuels. Although ignition was obtained at this condition, its character was dramatically different from what was observed at higher equivalence ratios in that no visible flame was produced. Instead, the ignition was marked by an audible deflagration of sufficient strength to raise the reactor cover. Although there was no flame, the ignition event resulted in the same sudden temperature increase observed in other cases. As shown in Table 1, one test was conducted with octane below the lean flammability limit. At an equivalence ratio of 0.4, the mixture could not be ignited with a foil temperature as high as 1120°C. The test results indicate then that the ignition temperature remains fairly constant over a wide range of equivalence ratios and exhibits a virtual discontinuity at the lean limit.

4.3.3 Vapor Phase Ignition Delay Time

Although a large number of tests were conducted, most resulted in ignition delay times which were too short to measure; that is, the ignition event occurred during the initial period required to heat the foil to the equilibrium temperature. The most consistent and useful data on delay time were obtained with the largest foil tested. These results for hexane are shown in Figure 24 plotted in the form suggested by Equation 54. The data exhibit no clear trend with equivalence ratio indicating even less sensitivity to this parameter than was observed in the case of ignition temperature. The straight-line correlation of the data corresponds to Equation 54 arbitrarily evaluated at the stoichiometric condition. The values of $E/R = 19,000^\circ\text{K}$ and $A = 1.8 \times 10^{13} \text{ cm}^3/\text{gm mole sec}$ were obtained from a least-squares fit to the data which resulted in a very satisfactory correlation coefficient of around 0.83. In addition, the correlating values of E/R and A are remarkably close to the corresponding values obtained in the application of the model to the ignition temperature data.

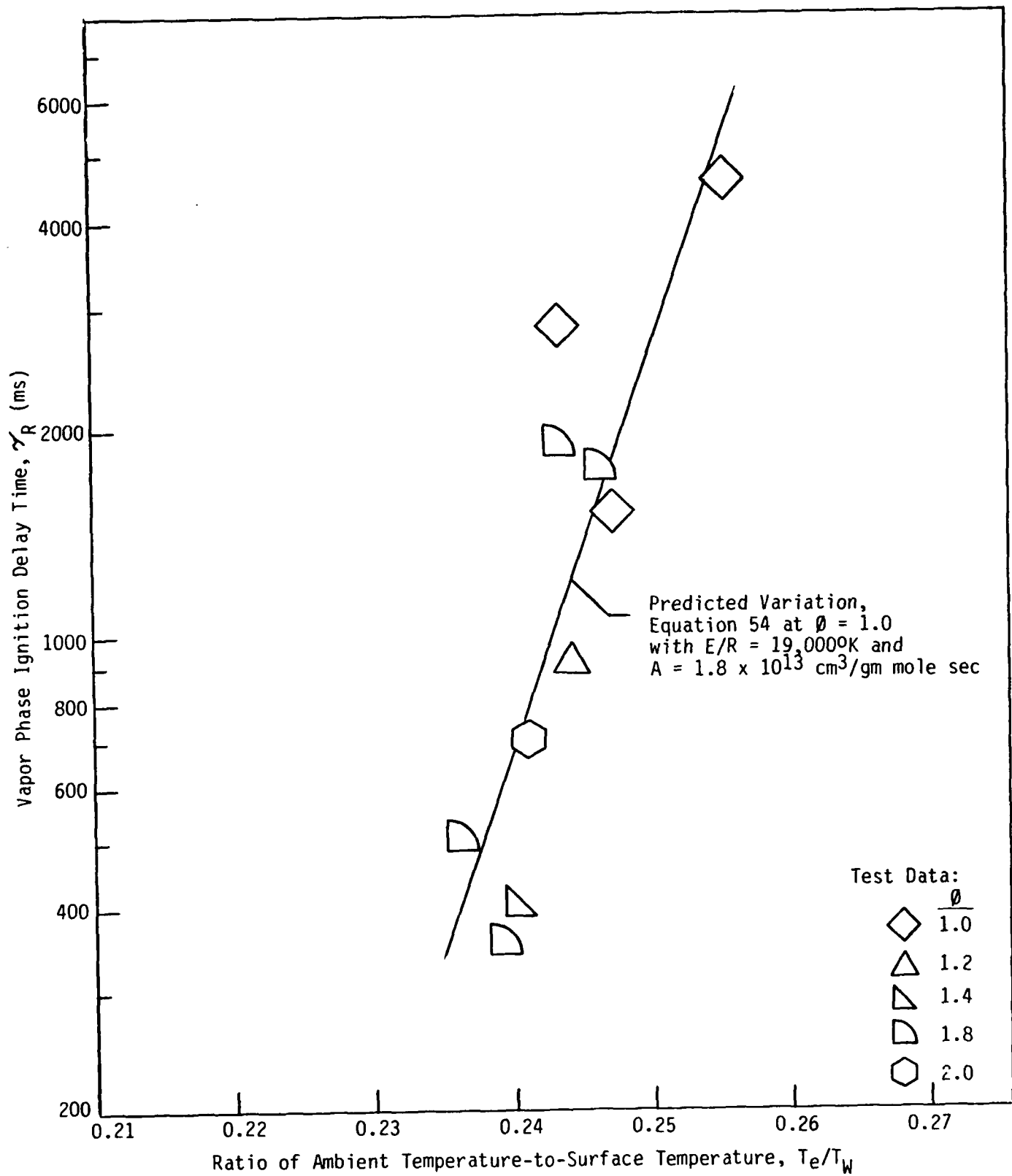


Figure 24. CORRELATION OF VAPOR PHASE IGNITION DELAY TIME FOR HEXANE WITH 9.52 mm FOIL

One obvious shortcoming of the transient model is that it predicts that surface size has no effect on the vapor-phase ignition delay time. The limited amount of data obtained with the smallest foil and presented in Figure 25 demonstrate that this is not true. The relatively large amount of scatter in these results is apparently related to the difficulty which was encountered in setting and maintaining a constant temperature with the small foil due to its comparatively low electrical resistance. Despite the scatter, however, it is apparent that the delay time at a given temperature increases with decreasing surface size.

Although the transient model does not predict the effects of all parameters, its success in correlating so well the test data for the large foil is very encouraging. The results obtained indicate strongly that it provides a satisfactory representation of the important mechanisms.

4.4 Ignition of Liquid Fuel/Air Mixtures

4.4.1 Spray Characteristics

The final portion of the experimental investigation focused on determining the effects of a liquid phase on the hot-surface ignition phenomenon. All of the testing was conducted for the specific case where the fuel is in the form of a spray from a conventional swirl-type atomizer. Data were obtained with two atomizers of different flow capacity (orifice size) both of which produced solid-cone sprays with 80° cone angles. Theoretically, the only difference in the spray characteristics would be in the mean drop diameter. Unfortunately, measurement of drop size was beyond the scope of the present investigation.

Although the characteristic drop size for the two sprays tested cannot be determined exactly, an order-of-magnitude estimate can be obtained using existing correlations for similar configurations. A generally accepted correlation which applies to well-designed swirl-type pressure nozzles which produce a hollow-cone spray is as follows:

$$SMD = 160 \frac{C_N^{0.25}}{P_I^{0.15}} \quad (61)$$

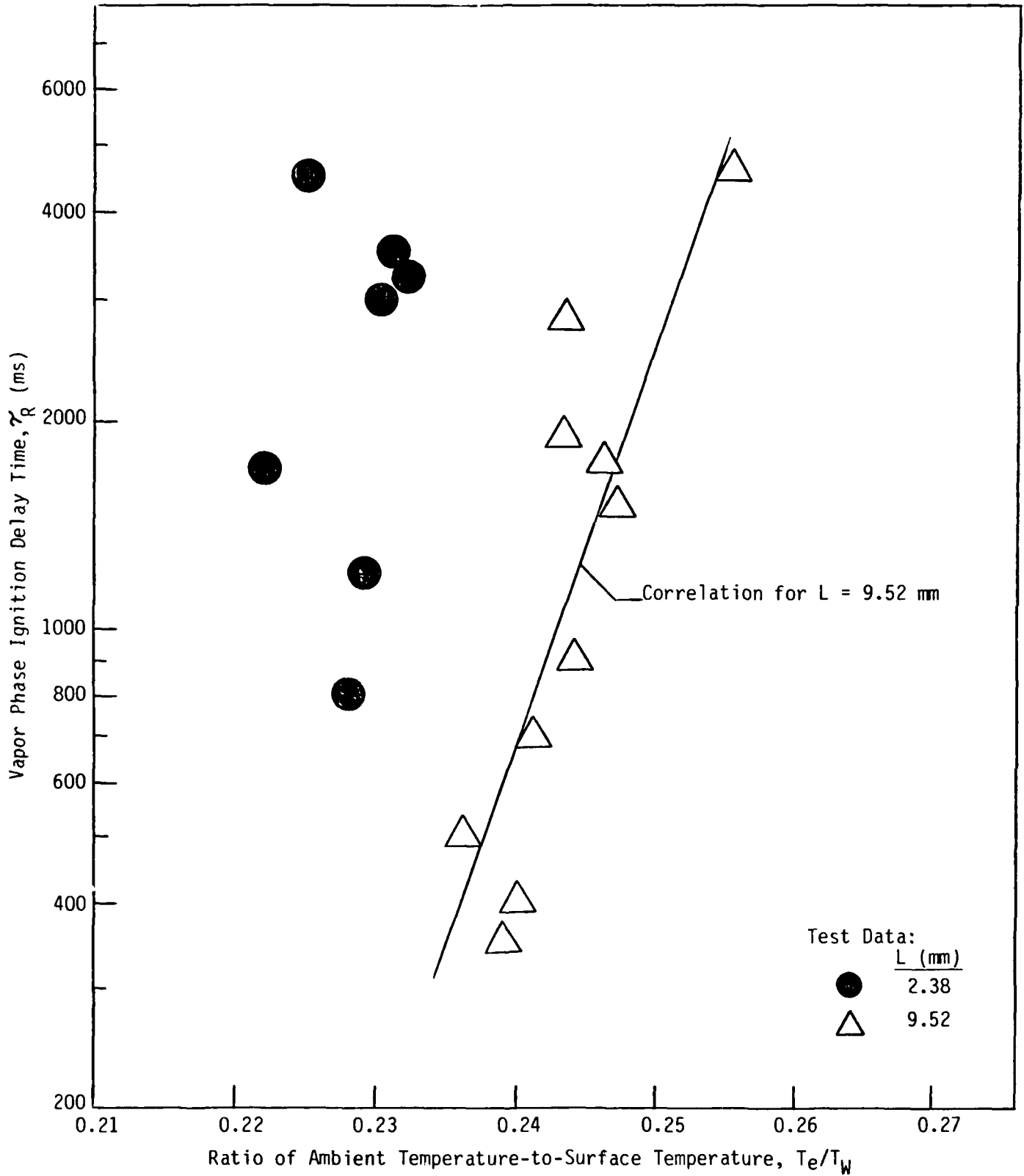


Figure 25. EFFECT OF SURFACE SIZE ON IGNITION DELAY TIME FOR HEXANE

where SMD is the Sauter mean diameter in microns, C_N is the nozzle flow capacity in GPH, and P_I is the fuel injection pressure in psi.

The injection method used should theoretically provide a fuel pressure of around 7 times the air pressure applied to the piston. Because of the large amount of friction associated with the O-ring seals, however, the actual injection pressure was less than the theoretical value. Based on measurements, it was estimated that fuel injection pressure was in the 70-360 psi range over the corresponding range of applied air pressures tested. Substitution of these values in Equation 61 gives an estimated SMD of 60-70 microns for the 0.6 GPH atomizer and 85-110 microns for the 2.75 GPH atomizer. The expected effect of pressure then appears to be negligible.

The above estimates correspond to a correlation which is strictly applicable to hollow-cone atomizers. It is generally known that solid-cone atomizers produce a larger SMD than a comparable hollow-cone design. In addition, the characteristic of the solid spray is that the largest drops tend to be concentrated around the centerline. On the basis of these considerations, it would be expected that the effective mean spray drop sizes obtained in the ignition tests should be on the same order but somewhat larger than the estimated values of SMD.

4.4.2 Details of Ignition Process

For a given spray, an increase in the hot-surface temperature should decrease the time required to achieve ignition. This effect is illustrated by the typical results presented in Figure 26 which show the measured time-temperature trace in terms of phototransistor output for two different foil temperature levels. At the lower temperature, ignition occurs approximately 400 ms after the spray reaches the foil. As can be seen, an order-of-magnitude decrease in delay time occurs when the temperature is increased by approximately 70°C.

The effect of drop size can be examined by comparing the ignition results obtained with the two different atomizers at approximately the same surface temperature as shown in Figure 27. For both atomizers the

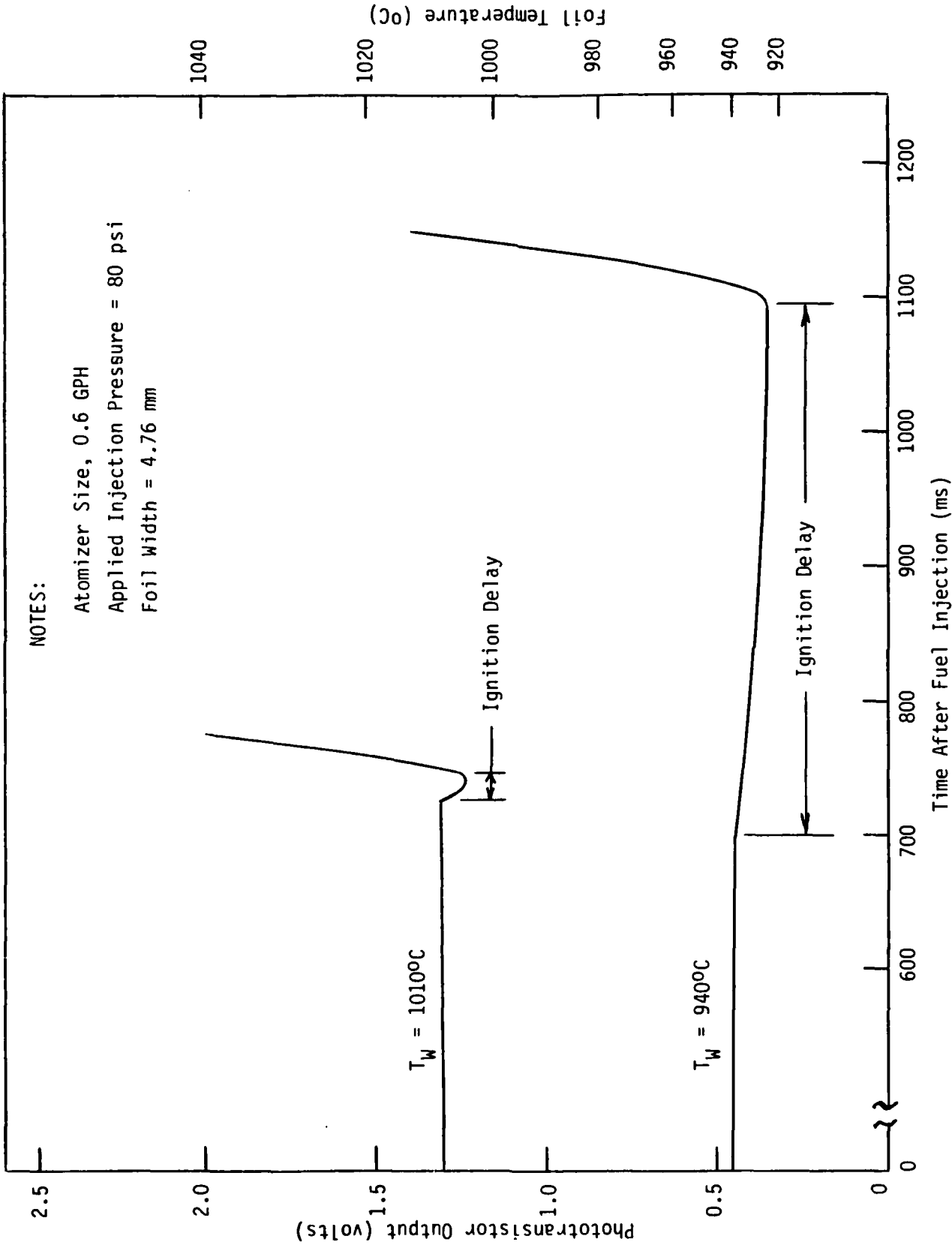


Figure 26. TYPICAL EFFECT OF HOT-SURFACE TEMPERATURE ON SPRAY IGNITION DELAY TIME FOR OCTANE

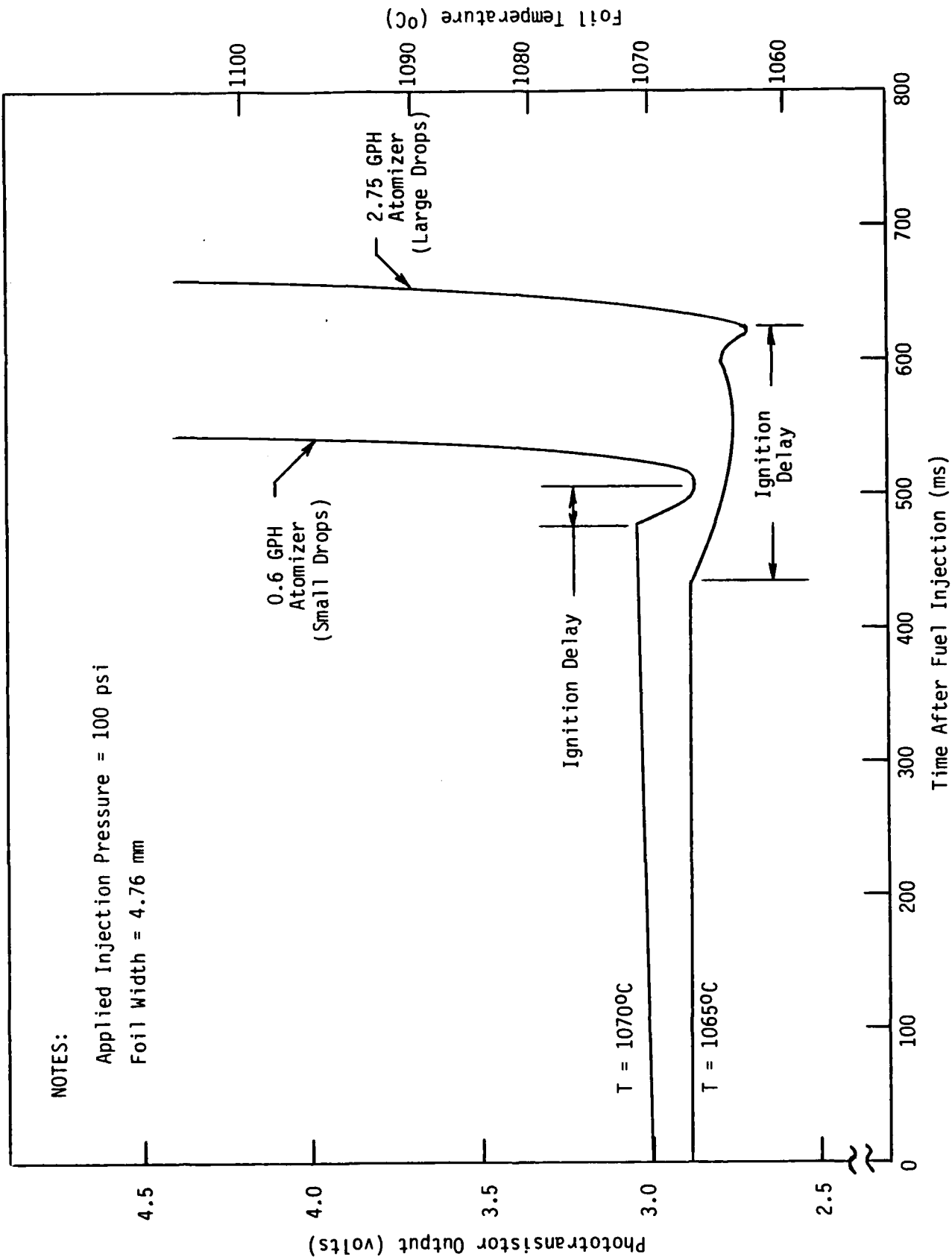


Figure 27. TYPICAL EFFECT OF DROP SIZE ON SPRAY IGNITION DELAY TIME FOR OCTANE

spray reaches the vicinity of the foil at about the same time. However, ignition occurs significantly later with the 2.75 GPH atomizer. The observed increase in delay time is related to the characteristically longer vaporization time associated with the larger droplets produced by this atomizer. These results provide a good demonstration of the typical manner in which the overall ignition process is influenced by the presence of a liquid phase.

4.4.3 Correlation of Spray Ignition Delay Time

The experimentally determined values of overall ignition delay time for the 0.6 GPH atomizer are plotted versus surface temperature in Figure 28. The injection pressure appears to have a negligible effect on the results obtained. This confirms the expected insensitivity of drop size to injection pressure. Above a surface temperature of around 950°C, the data are quite consistent. The increased amount of scatter below this temperature is associated with the fact that in this region the vapor-phase reaction time constitutes the major component of the total delay time. The essentially exponential variation of this component with temperature is difficult to measure accurately.

The broken curves superimposed on the experimental data represent the predicted variations of the individual contributions to the total delay time (τ_I) associated with the liquid phase ($\tau_L = \tau_V + \tau_M$) and the vapor-phase reaction (τ_R). These were obtained by applying the transient model (as constituted by Equations 54-56) assuming stoichiometric conditions and adjusting the values of E, A, and a_0 to provide an acceptable fit to the data. As can be seen, the correlation indicates a mean effective drop size of around 150 microns which is quite realistic in comparison to the estimated values of SMD discussed previously. The empirical values of $E/R = 19,000^\circ\text{K}$ and $A = 4.4 \times 10^{13} \text{ cm}^3/\text{gm mole sec}$ also agree fairly well with the corresponding values previously obtained in correlating the vapor phase ignition data.

The application of the model to the test results for the 2.75 GPH atomizer is shown in Figure 29. In this case, the correlation indicates a mean drop size of about 350 microns which again is fairly realistic. In addition, the relative magnitude compared to the 0.6 GPH nozzle is close

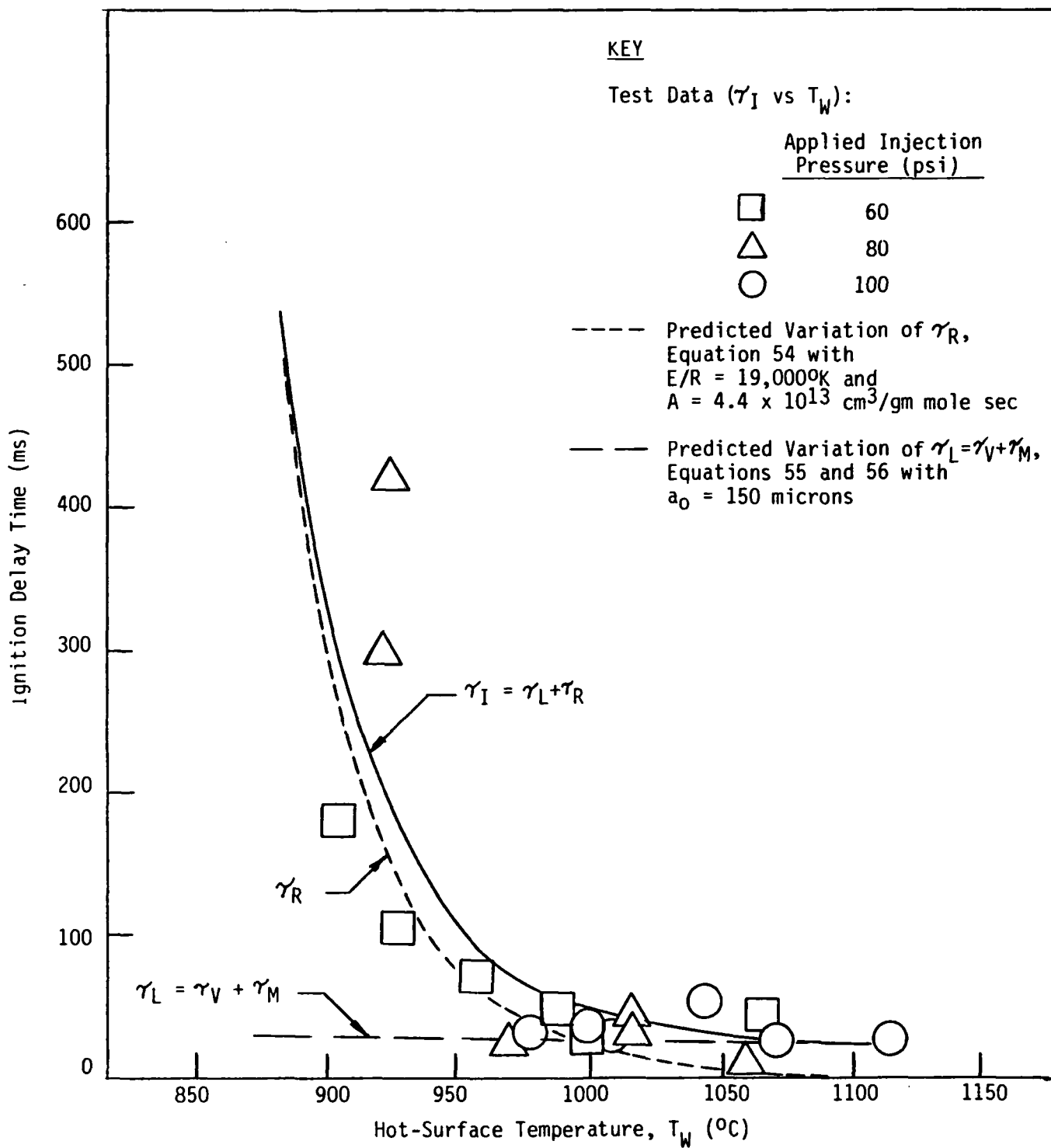


Figure 28. CORRELATION OF OCTANE SPRAY IGNITION TEST RESULTS FOR 0.6 GPH ATOMIZER

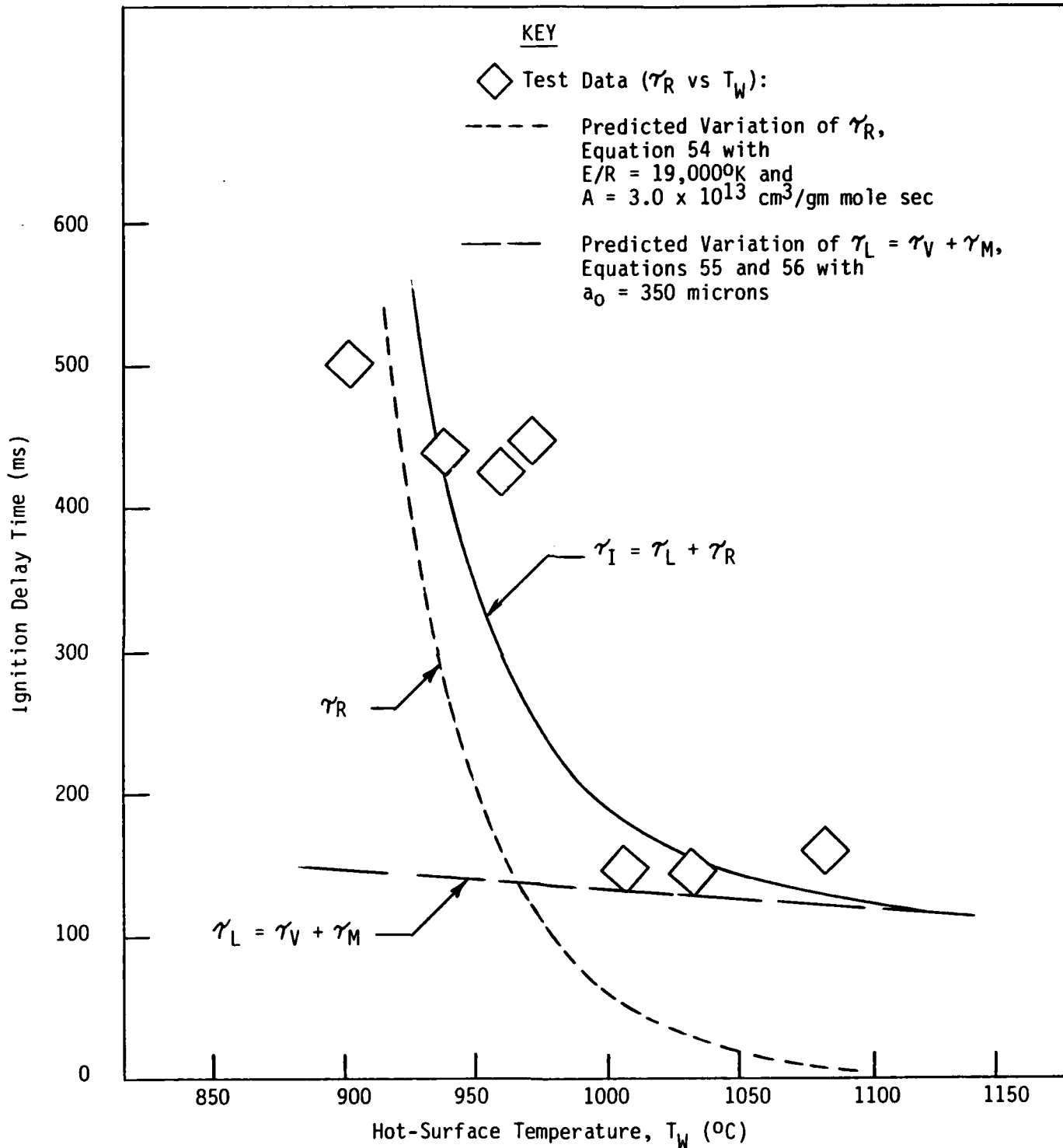


Figure 29. CORRELATION OF OCTANE SPRAY IGNITION TEST RESULTS FOR 2.75 GPH ATOMIZER

to what is predicted by the approximate SMD correlation. Although the empirical value of activation energy is the same as obtained with the 0.6 GPH atomizer, a slightly lower value of A is indicated. This would not appear to be a significant discrepancy considering the limited amount of data for the larger atomizer.

The overall effects of surface temperature and drop size on spray ignition are illustrated in Figure 30 which is a composite plot of all of the test data. The superimposed curves represent the correlations of total ignition delay time obtained in applying the model. The projected variations indicate a minimum ignition temperature in the 850-950°C range. This is confirmed not only by the results presented in Table 2 for those tests where no spray ignition was obtained but also by the vapor-phase ignition data for octane shown in Figure 23. In general then the correlations appear to match quite well the observed trends.

4.5 Model Assessment

The analytical model has been utilized to correlate successfully the experimental ignition data over wide ranges of a significant number of test parameters. Despite its simplicity, the model seems to provide a satisfactory representation of the important ignition mechanisms for both vaporized and liquid fuels. In addition, the good agreement between predicted and experimentally observed trends has been obtained with remarkably few empirical constants. The overall results obtained clearly demonstrate the validity of the basic analytical approach as well as its practical utility in correlating experimental ignition data.

Table 2
SUMMARY OF EXPERIMENTAL IGNITION RESULTS
FOR SPRAYS OF LIQUID OCTANE IN AIR⁽¹⁾

Test No.	Atomizer Flow Capacity (GPH)	Applied Air Injection Pressure (psig)	Preheat Time (sec) ⁽²⁾	Ambient Reactor Temperature T_e (°C)	Foil Temperature T_w (°C)	Total Ignition Delay Time γ_I (ms)
1	0.6	60	5	24	1075	40
2	0.6	60	5	24	1010	30
3	0.6	60	5	24	1000	50
4	0.6	60	5	26	975	70
5	0.6	60	5	25	945	110
6	0.6	60	5	25	920	180
7	0.6	60	5	25	895	5000+(3)
8	0.6	80	5	--	1075	10
9	0.6	80	5	25	1035	40
10	0.6	80	5	24	1010	40
11	0.6	80	5	25	990	30
12	0.6	80	5	25	940	420
13	0.6	80	5	25	920	5000+(3)
14	0.6	80	15	--	1015	30
15	0.6	80	15	--	920	300
16	0.6	80	15	--	920	5000+(3)
17	0.6	80	15	--	890	5000+(3)
18	0.6	100	5	16	1090	30
19	0.6	100	5	21	1070	30
20	0.6	100	5	23	1050	60
21	0.6	100	5	23	1005	30
22	0.6	100	5	24	990	40
23	0.6	100	5	17	990	30
24	0.6	100	5	25	955	5000+(3)
25	2.75	100	5	18	1065	160
26	2.75	100	5	20	1025	140
27	2.75	100	5	22	1010	130
28	2.75	100	5	23	975	450
29	2.75	100	5	21	960	420
30	2.75	100	5	23	945	440
31	2.75	100	5	24	910	500
32	2.75	100	5	23	890	5000+(3)

- NOTES:
1. All tests conducted with 4.76 mm foil and nominal overall equivalence ratio of 1.0.
 2. Foil heating time prior to fuel injection.
 3. No ignition was achieved in these tests.

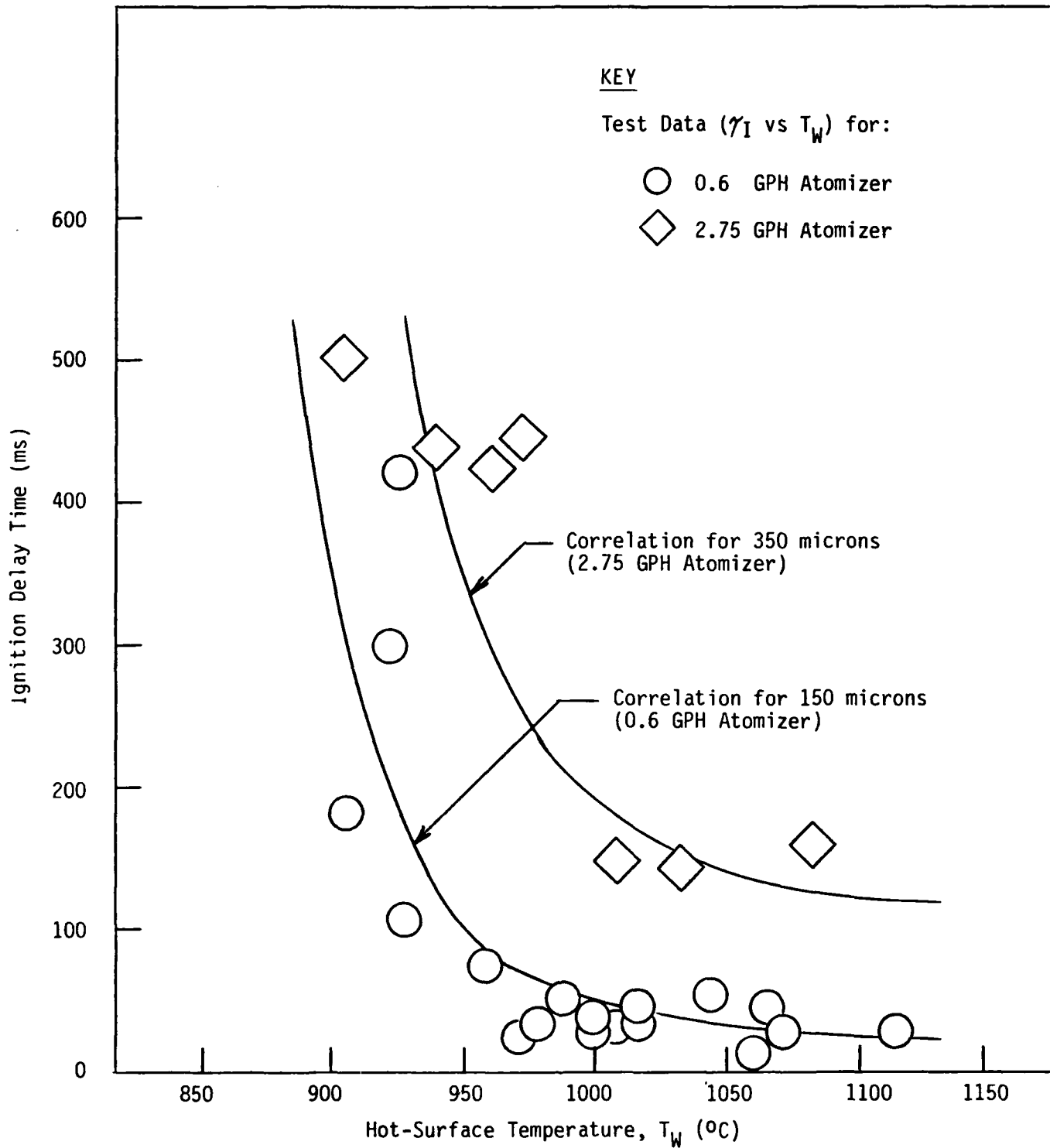


Figure 30. VARIATION OF OCTANE SPRAY IGNITION DELAY TIME WITH SURFACE TEMPERATURE AND DROP SIZE

5. CONCLUSIONS

A combined analytical and experimental study has been performed to investigate the ignition of combustible liquids by contact with hot surfaces. A total of over 120 tests were conducted to measure the minimum surface ignition temperature and ignition delay time for hexane and octane over a wide range of conditions. A simple analytical model of the hot-surface ignition phenomenon was developed and successfully applied in correlating the test data. On the basis of the overall results obtained, the following general conclusions can be made:

- For a given fuel and surface size, the ignition temperature is surprisingly insensitive to mixture composition although a weak minimum is observed at stoichiometric conditions.
- The ignition temperature increases by around 60°C when the surface size is reduced by a factor of four.
- The ignition delay time is strongly dependent on surface temperature and somewhat less sensitive to size.
- For the case of vaporized fuel, the ignition temperature of octane is around 50°C lower than the corresponding value for hexane. The general variation with mixture composition is essentially the same for both fuels.
- The ignition temperature for liquid sprays is approximately the same as for the case of vaporized fuel.
- The delay time for spray ignition varies with surface temperature in a predictable manner. At high temperatures it is roughly constant and equal to a value which is dependent on drop size due to the dominant effects of vaporization and mixing on the ignition process. As the temperature is reduced, vapor-phase reaction assumes the dominant role and the delay time increases dramatically.

- The simple analytical ignition model has been successful in correlating the test data particularly in predicting the effects of major parameters such as surface temperature on the conditions required for ignition. The model provides good agreement between predicted and experimentally-observed trends without requiring an extensive amount of empirical adjustment.

The test results have shown that the selected experimental technique is an extremely effective method of obtaining detailed and useful information on the phenomenon of hot-surface ignition. The initial success achieved in applying the analytical model to the experimental data has demonstrated the validity of the basic approach. The model offers significant promise in providing a practical design and analysis tool for dealing with the potential hazards associated with combustible liquids.

6. RECOMMENDATIONS

Based on the encouraging results obtained to date, it is strongly recommended that an expanded investigation of the hot-surface ignition phenomenon be conducted as a Phase II study under the SBIR program. The recommended study should focus on further refining the analytical and experimental techniques developed in the present investigation.

The existing apparatus should primarily be modified to allow testing on a somewhat larger scale. In addition, it should include provisions for introducing combustible liquids in a variety of forms such as a jet, for example. The experimental facility should then be used in conducting a comprehensive investigation of a variety of practical liquids covering a wider range of conditions than was possible in the Phase I study.

A companion analytical effort should be conducted to further refine the simple ignition model. This effort should concentrate on improving the predictive ability of the model in those areas which have been identified in developing the current formulation. The objective should be to develop a general correlation based on detailed experimental data which can be applied with confidence in determining optimum safety measures for practical systems.

7. REFERENCES

1. Laurendeau, Normand M., "Thermal Ignition of Methane-Air Mixtures by Hot Surfaces: A Critical Examination," The Combustion Institute, Combustion and Flame 46:29-49 (1982).
2. Laurendeau, N.M. and Caron, R.N., "Influence of Hot Surface Size on Methane-Air Ignition Temperature," The Combustion Institute, Combustion and Flame 46:213-218 (1982).
3. Laurendeau, N.M., "The Feasibility of Methods and Systems for Reducing LNG Tanker Fire Hazards," Report DOE/EV/04734-T1 (DOE Contract EP-78-C-02-4734.A000) (1980).
4. Treybal, Robert E., "Mass-Transfer Operations," McGraw-Hill Book Company, Inc. (1955).
5. Giedt, Warren H., "Principles of Engineering Heat Transfer," D. Van Nostrand Company, Inc., Princeton, NJ.
6. Ibid, pg. 149.
7. Ibid, pg. 308.

END

FILMED

3-86

DTIC